Study of Electromagnetic Wave Scattering from Rough Icy Surfaces

Dissertation submitted in partial fulfillment of the requirements for the degree of

Master of Technology

in

Opto-Electronics and Optical Communication

Submitted by

Akashdeep Bansal

2014JOP2485

Under the supervision of

Dr. Uday K Khankhoje

Department of Electrical Engineering

Indian Institute of Technology Delhi

July, 2016

Certificate

This is to certify that the following dissertation titled "Study of electromagnetic wave scattering from rough icy surfaces", submitted by Mr. Akashdeep Bansal, Entry No. 2014JOP2485 in partial fulfillment of the academic requirements of the course JOD802, M.Tech Project represents bonafide work done under my supervision. It has not been submitted elsewhere to the best of my knowledge.

Dr. Uday K Khankhoje
Dept. of Electrical Engineering
Indian Institute of Technology, Delhi
New Delhi - 110016

Acknowledgements

I thank my Supervisor Dr. Uday K Khankhoje for his guidance and for giving me the opportunity to work on this project. Your valuable suggestions and the fruitful discussions were the source for the project to progress continuously. Apart from the project, you have been an excellent mentor also. I am thankful for all the advice you have given regarding my career.

I am very thankful to my lab colleagues Nitin K. Lohar, Yaswanth Kalapu and Sayak Bhattacharya for providing such friendly environment in the lab. Specially for Nitin K Lohar, I really appreciate the encouragement you have given me whenever I was feeling down. I would like to thank my classmates Kandlagunta Sridhar Reddy for making this journey memorable. I would also like to thank my family for their support and inspiration.

Akashdeep Bansal
IIT Delhi
June, 2016

Abstract

We present a semi-analytical, second-order perturbative solution to the problem of electromagnetic plane wave scattering from a dielectric medium with a randomly rough surface using the small perturbation approach. Using the results, we have analysed different type of icy surfaces on the basis of Radar cross section (RCS) and Circular Polarisation Ratio (CPR). And we found that random rough surface with boulders like configuration may explain the high radar albedo and CPR from Enceladus.

Contents

1 Introduction **1**

2 Analysis of Random Rough Surfaces using SPM **3**
2.1 Small Perturbation Method 3
2.1.1 Extinction Theorem 3
2.1.2 Green's Function 5
2.1.3 Assumptions in analysis 6
2.2 Boundary Conditions 6
2.3 Analysis using SPM 7
2.3.1 Zeroth Order 8
2.3.2 First order 9
2.3.3 Second order 10

3 Scattered Field from Random Rough Surfaces **13**
3.1 Scattered Field 13
3.1.1 Zeroth Order 13
3.1.2 First Order 14
3.1.3 Second Order 15
3.2 Scattered Field as a Function of Incident and Scattered Angles 17
3.2.1 Zeroth Order 18
3.2.2 First Order 19

4 Ice Configurations: Analysis using RCS and CPR **24**
4.1 Radar Cross Section (RCS) 24
4.2 Circular Polarisation Ratio (CPR) 25
4.3 Analysis using Radar Cross Section 25
4.3.1 Random Rough Surface 25
4.3.2 Random Rough Surface with Boulders 27
4.4 Analysis using CPR 29
4.4.1 Random Rough Surface 30
4.4.2 Random Rough Surface with Uniformly Distributed Smooth Square Boulders 32

5 Conclusion **35**

A Green's Function and Its Gradient **37**

B Auto Correlation Function of a Random Rough Surface 39

List of Figures

2.1 An inhomogeneous medium composed of two homogeneous mediums. . 4
2.2 An electromagnetic wave falling on a random rough horizontal surface. 5

3.1 Decomposition of propagation vectors along x- and z-axes 17
3.2 Zeroth order Reflected power in specular direction for TE polarisation as a function of the incident angle, θ_i 19
3.3 Zeroth order reflected power in specular direction for TM polarisation as a function of the incident angle, θ_i 20
3.4 First order scattered power for TE polarisation as a function of the scattering angle, θ_s at incident angle, $\theta_i = 40°$ ensemble averaged over 1000 surfaces. 21
3.5 First order scattered power for TE polarisation as a function of the scattering angle, θ_s at incident angle, $\theta_i = 40°$. 21
3.6 First order scattered power for TM polarisation as a function of the scattering angle, θ_s at incident angle, $\theta_i = 40°$ ensemble averaged over 1000 surfaces. 22
3.7 First order scattered power for TM polarisation as a function of the scattering angle, θ_s at incident angle, $\theta_i = 40°$. 23

4.1 Backscattering phenomenon from random rough surface 26
4.2 Backscatter Power variation as a function of Monostatic Radar viewing angle for TE polarisation. 26
4.3 Backscatter Power variation as a function of Monostatic Radar viewing angle for TM polarisation. 27
4.4 Backscattering phenomena from random rough Surface with smooth boulder 27
4.5 Backscatter Power variation as a function of Boulder factor (α) for TE polarisation at an incident angle of 40°. 29
4.6 An RHCP electric field is incident on a random rough surface. 31
4.7 The variation of the backscatter CPR from random rough surface with incident angle w.r.t. normal to the surface. 31
4.8 The variation in CPR w.r.t. the incident angle assuming both surface and boulder as smooth. 33
4.9 Variation in backscatter CPR from a random rough surface as a function of the rms height of the rough surface,h, keeping correlation length,l, constant. 34

4.10 Variation in Backscatter CPR from a random rough surface as a function of the auto correlation length,l, of the rough surface keeping rms height,h, constant 34

Chapter 1

Introduction

Humans are continuously trying to search for life on planets other than the Earth of the Solar system. This has led to the emergence of the field for searching water/ice on celestial bodies. Not only this, they are also highly curious about knowing the facts behind the formation of the Solar system.

The curiosity of human towards the celestial bodies has led to the growth of the field known as "Remote Sensing". *Remote sensing is defined as obtaining information about any object without any physical contact with it* [1]. The object can be on Earth or may be on other celestial bodies of the universe. Radar (RAdio Detection And Ranging) is one of the important instruments used in remote sensing. During radar scan, it is observed that some of the celestial bodies having ice on their surface give very high radar albedo as compared to the North and South pole of the Earth. One amongst them is the Enceladus (moon of the Saturn) [2] [3]. This leads to a mystery, why are we getting high radar albedo from the Enceladus?

To understand this, we first have to understand the interaction of the electromagnetic waves with the random rough surfaces. The analysis of electromagnetic wave scattering from random rough surfaces has its roots in classical works of the previous two centuries. This field is highly important for remote sensing, communications, oceanography, optics and material science.

Early approaches for analysing the electromagnetic wave scattering from the random rough surfaces are based on asymptotic approximations like small-perturbation method (SPM) by Rice [4], Kirchoff or tangent plane approximation (KA), phase perturbation method (PPM), small-slope approximation (SSA), momentum transfer expansion (MTE), unified perturbation method (UPM) and the integral equation model (IEM) [5].

Due to a large number of applications, this was the field of interest continuously and lot of work was done in finding the domain of validity region for various analytical techniques, like for Kirchoff approximation by Thoros [6]. These methods are analytical, hence highly useful in understanding the physical insight of the interaction.

Due to tedious manual calculations, lack of accuracy and limited domain of validity of analytical techniques, some numerical techniques were developed like method of moments (MOM), finite difference time domain (FDTD) and finite element method (FEM).

In [7], Johnson observed polarisation dependence of electromagnetic wave scattering from random rough surfaces and depolarisation of electromagnetic waves was observed by Valenzuela [8]. In [9], it was observed that Lunar crater deposits exhibit maximum CPR (Circular Polarisation Ratio, μ_c) values of 2 to 3 at 12.6 and 70-cm wavelengths, Maxwell Montes on Venus range up to about 1.5 at 12.6-cm wavelength, Echoes from SP Flow in Arizona exhibit values up to 2 at 24-cm wavelength, rock edges and cracks (dipole-like) produce μ_c of unity for single scattering and up to about 2 for multiple reflections, Natural corner reflectors (dihedrals) formed by pairs of rock facets can yield an average value of 3 to 4. The CPR is defined as "the ratio between power reflected in the same sense of circular polarisation (SC) as that of transmitted and the echo in the opposite sense (OC) of circular polarisation" [9].

In [2], the authors through 2D FEM (finite element method) analysis show that highly porous substrates, possibly combined with nearly circular pebbles of ice atop can explain the high radar albedo from the Enceladus.

The above researches in the past have given the idea that different configurations of ice will generate different scattered electromagnetic field and will provide different values of radar cross section (RCS) and circular polarisation ratio (CPR). The RCS is defined as the ratio of the reflected radiation from the surface to incident radiation upon it.

Objective

To categorise different configurations of icy surfaces on the basis of two parameters: radar cross section (RCS) and circular polarisation ratio (CPR). Finally, to solve the mystery of getting high radar albedo from icy celestial bodies like Enceladus than the North/South pole of the Earth.

Organisation of the thesis

In Chapter 2, we analyse electromagnetic wave scattering from random rough surfaces by using small perturbation method (SPM) with a continuation in Chapter 3, derivation of scattered field for different orders of perturbation of the height of random rough surfaces. In Chapter 4, we analyse two configurations of icy surfaces: random rough surface and random rough surface with smooth square boulders, on the basis of RCS and CPR. In Chapter 5, we end our discussion with a conclusion.

Chapter 2

Analysis of Random Rough Surfaces using SPM

In this chapter, we develop the basic understanding of small perturbation method (SPM) [4] [10]. We solve the second-order partial differential equation (Helmholtz wave equation), derived from Maxwell's differential equations, using SPM, extinction theorem [11] and Green's function.

2.1 Small Perturbation Method

Small perturbation method (SPM) is a traditional approach for analysing the electromagnetic wave scattering from random rough surfaces. This is semi analytical, asymptotic approximation based technique for solving complex Maxwell's differential equation using boundary conditions. This technique was given by Rice in 1951 [4]. This approach is valid only for slightly rough surfaces, i.e., low frequency of randomness of the surface [12] [5].

In SPM, we expand the unknown fields at the interface into terms of different orders of the height of random rough surface, $f(x)$, similar to the Taylor series expansion:

$$g(p+r) = g(p) + r\ g'(p) + \frac{r^2}{2!} g"(p) + \cdots$$

where, and then we compare the different order terms to get an approximate value of the unknown field parameters at the interface.

2.1.1 Extinction Theorem

In practical situations, we do not find homogeneous media. To determine the field expressions in a medium, we need to solve wave equation in that medium. To solve the wave equation in an inhomogeneous medium requires some technique to avoid complexity and tediousness of mathematical calculations. If the inhomogeneties are piecewise constant for each region, then we can use the surface integral equation technique [11]. In this technique, the homogeneous-medium Green's functions are found for each region. Then, the field in each region is written in terms of the field due to any

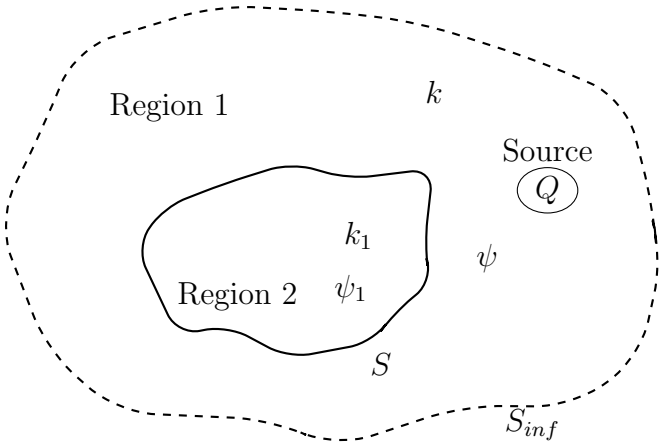

Figure 2.1: An inhomogeneous medium composed of two homogeneous mediums [1].

sources in the region plus the field due to surface sources at the interfaces between the regions, following Huygens' principle. Next, the boundary conditions at these interfaces are used to set up integral equations known as surface integral equations. Then these equations can be solved to get the unknown surface sources at the interface.

Let us assume an inhomogeneous medium composed of two homogeneous mediums with ψ and ψ_1 be the total fields in medium 1 and 2, respectively, as shown in Fig. 2.1. In region 1, the field will be due to source Q and the surface sources at the interfaces due to the field in region 2. Similarly, in region 2, the field will be due to the surface sources at the interface due to field in region 1. And these fields will be zero in opposite regions. Now, on solving the Helmholtz wave equation using homogeneous green's function $g(r, r')$ and $g_1(r, r')$ for region 1 and 2, respectively, we get

$$Q(\overrightarrow{r}') - \int_s ds\ \hat{n} \cdot \left[g(\overrightarrow{r}, \overrightarrow{r}')\nabla\psi(r) - \psi(r)\nabla g(\overrightarrow{r}, \overrightarrow{r}') \right] = 0, \text{ for region 2} \quad (2.1)$$

$$\int_s ds\ \hat{n} \cdot \left[g_1(\overrightarrow{r}, \overrightarrow{r}')\nabla\psi_1(r) - \psi_1(r)\nabla g_1(\overrightarrow{r}, \overrightarrow{r}') \right] = 0, \text{ for region 1} \quad (2.2)$$

where,

$$\begin{aligned} \psi, \psi_1 &= \text{Total field in medium 1 and 2, respectively} \\ Q &= \text{Source field in medium 1} \\ \hat{n} &= \text{Unit normal vector at the medium interface} \end{aligned}$$

Now, on applying to our problem statement, where a field ψ_{inc} is falling on a random rough surface separating two semi-infinite upper and lower dielectric mediums with dielectric constants ϵ and ϵ_1, respectively, as shown in Fig. 2.2, we get

$$\psi_{inc}(\overrightarrow{r}') + \int_s dx\ \left[a(x)\sqrt{1 + (\frac{df}{dx})^2}\hat{n} \cdot \nabla g(\overrightarrow{r}, \overrightarrow{r}') - g(\overrightarrow{r}, \overrightarrow{r}')\ \eta\ b(x) \right] = 0, \text{ for } z' < f(x') \quad (2.3)$$

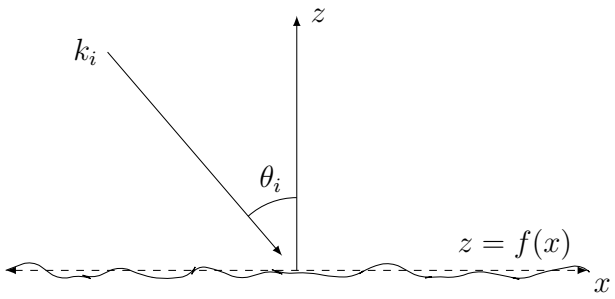

Figure 2.2: An electromagnetic wave falling on a random rough horizontal surface [10].

$$\int_s dx \left[a(x)\sqrt{1+(\frac{df}{dx})^2}\hat{n}\cdot\nabla g_1(\overrightarrow{r},\overrightarrow{r'}) - g_1(\overrightarrow{r},\overrightarrow{r'})\ b(x)\right] = 0,\ \text{for } z' > f(x'), \quad (2.4)$$

where,

$$\hat{n} = \frac{1}{\sqrt{1+(\frac{df}{dx})^2}}\left(-\frac{df}{dx}\hat{x}+\hat{z}\right)$$

$$\eta = \begin{cases} 1, & \text{TE Polarisation} \\ \frac{\epsilon}{\epsilon_1}, & \text{TM Polarisation} \end{cases}$$

$$a(x) = \psi_1(x, f(x))$$

and

$$b(x) = \sqrt{1+\left(\frac{df}{dx}\right)^2}\left[\hat{n}\cdot\nabla\psi_1(\overrightarrow{r})\right]_{z=f(x)}$$

$a(x)$ and $b(x)$ are known as surface field unknowns. The second term in the Eq. (2.3) is giving us the scattered field due to random rough surface. $g(\overrightarrow{r},\overrightarrow{r'})$ and $g_1(\overrightarrow{r},\overrightarrow{r'})$ are the Green's function in upper and lower dielectric medium.

2.1.2 Green's Function

Green's function is defined as the field in a medium due to point source i.e., it is the solution of the second order partial differential equation (Helmholtz equation), derived from the Maxwell's equation, where the driving force is a unit source (Dirac delta or impulse function). i.e.,

$$\nabla^2 g(r,r') + \omega^2\mu\epsilon g(r,r') = -\delta(r-r')$$

where ∇^2 is Laplace operator, ω is angular frequency of the wave, μ amd ϵ be the magnetic permeability and electrical permittivity of the medium, respectively. In 2D, the solution of the Helmholtz equation with a Dirac delta function is given by Hankel

function, whose plane wave representations for the $g(\overrightarrow{r}, \overrightarrow{r}')$ and $g_1(\overrightarrow{r}, \overrightarrow{r}')$ are given by [13]

$$g(\overrightarrow{r}, \overrightarrow{r}') = \frac{i}{4\pi}\int_{-\infty}^{\infty} dk_x \frac{1}{k_z}\exp[ik_x(x'-x)+ik_z|z'-z|] \tag{2.5}$$

$$g_1(\overrightarrow{r}, \overrightarrow{r}') = \frac{i}{4\pi}\int_{-\infty}^{\infty} dk_{1x} \frac{1}{k_{1z}}\exp[ik_{1x}(x'-x)+ik_{1z}|z'-z|] \tag{2.6}$$

where, $k_z = \sqrt{k^2-k_x^2}$, $k_{1z} = \sqrt{k_1^2-k_{1x}^2}$, k and k_1 be the propagation vector of the wave in upper and lower dielectric medium, respectively, with k_x, k_{1x} and k_z, k_{1z} are the respective components along x- and z-axes.

2.1.3 Assumptions in analysis

In the analysis, we have taken some assumptions to make calculations simpler and to satisfy the validity domain of the SPM, which are-

- 2D Geometry, i.e., randomness of surface is along one direction only with another dimension infinite.
- Zero mean, low rms height, h, and correlation length, l, satisfying SPM criterion $kh \leq 0.3$ and $\frac{h}{l} < \frac{17\pi}{180\sqrt{2}}$ [1].
- Homogeneous substrate to avoid effect of internal scattering.
- Randomness of the surface is assumed to have Gaussian auto correlation function, $C(x) = \exp(-x^2/l^2)$ and spectral density function, $W(k_x) = \frac{h^2 l}{2\sqrt{\pi}}\exp(-k_x^2 l^2/4)$

These are the reasonable assumptions for various geometries and hold valid for SPM analysis.

2.2 Boundary Conditions

In a 2D problem, consider an electromagnetic plane wave incident at an angle θ_i with the z axis, and the incident wavevector, k_i, being in the xz plane, falling on a random rough surface profile $z = f(x)$ separating two upper and lower non-magnetic, homogeneous, linear dielectric media with dielectric constants ϵ and ϵ_1, respectively, as shown in Fig. 2.2. The incident field, ψ_{inc}, may be expressed as

$$\psi_{inc}(\overrightarrow{r}) = \exp[i(k_{ix}x - k_{iz}z - \omega t)]\hat{y}$$

where $k_{ix} = k\sin\theta_i$ and $k_{iz} = k\cos\theta_i$, and ω is the angular frequency of the wave in upper dielectric.

Let ψ and ψ_1 be the field components directed along y-axis in upper and lower dielectric, respectively. So, the boundary conditions become

$$\psi(\overrightarrow{r}) = \psi_1(\overrightarrow{r})$$

and

$$\hat{n} \cdot \nabla\psi(\overrightarrow{r}) = \eta\ \hat{n} \cdot \nabla\psi_1(\overrightarrow{r})$$

where,

$$\eta = \begin{cases} 1, & \text{TE Polarisation} \\ \frac{\epsilon}{\epsilon_1}, & \text{TM Polarisation} \end{cases}$$

and

$$\hat{n} = \frac{1}{\sqrt{1 + (\frac{df}{dx})^2}} \left(-\frac{df}{dx}\hat{x} + \hat{z} \right)$$

2.3 Analysis using SPM

To analyse the electromagnetic wave scattering from random rough surfaces, we have to determine the field expressions in both the media. To obtain field expressions in both the media, we solve the Eqs. (2.3) and (2.4) to find the surface field unknowns, a(x) and b(x). We use the small perturbation method [14], for which we expand a(x) and b(x) into different order terms of the random rough surface profile, $f(x)$, as defined below

$$a(x) = a_0(x) + a_1(x) + a_2(x) + \cdots$$

and

$$b(x) = b_0(x) + b_1(x) + b_2(x) + \cdots$$

where, $a_i/b_i(x)$ is i^{th} order component of $f(x)$. On substituting $a(x)$ and $b(x)$ in Eqs. (2.3) and (2.4), we get

$$\exp(i(k_{ix}x' - k_{iz}z')) - \frac{1}{2}\int_{-\infty}^{\infty} dk_x \left[\exp(ik_x x' - ik_z z')\ \frac{1}{2\pi}\int_{-\infty}^{\infty} dx\ \exp(-ik_x x + ik_z f(x)) \right.$$
$$\left. \left[\left(\frac{df(x)}{dx}\frac{k_x}{k_z} + 1 \right) (a_0(x) + a_1(x) + a_2(x) + \cdots) + \frac{i\eta}{k_z}(b_0(x) + b_1(x) + b_2(x) + \cdots) \right] \right]$$
$$= 0 \qquad (2.7)$$

and

$$\frac{1}{2}\int_{-\infty}^{\infty} dk_{1x} \exp[ik_{1x}x' + ik_{1z}z'] \frac{1}{2\pi}\int_{-\infty}^{\infty} dx\ \exp(-ik_{1x}x - ik_{1z}f(x))\ \left[\left(\frac{-df(x)}{dx}\frac{k_{1x}}{k_{1z}} + 1 \right) \right.$$
$$\left. (a_0(x) + a_1(x) + a_2(x) + \cdots) - \frac{i}{k_{1z}} (b_0(x) + b_1(x) + b_2(x) + \cdots) \right] = 0 \qquad (2.8)$$

Now we will solve Eqs. (2.7) and (2.8) for different orders of $a(x)$ and $b(x)$ individually. Solution for the first three orders are as follows-

2.3.1 Zeroth Order

$a_0(x)$ and $b_0(x)$ are the zeroth order components of $a(x)$ and $b(x)$. Zeroth order implies that there in no perturbation on the surface, i.e., surface is perfectly smooth. So, we can put $f(x) = 0$. On comparing the zeroth order terms of Eq. (2.7), we get

$$\exp[i(k_{ix}x' - k_{iz}z')] - \frac{1}{2}\int_{-\infty}^{\infty} dk_x \ \exp[ik_x x' - ik_z z'] \ \frac{1}{2\pi}\int_{-\infty}^{\infty} dx \ \exp(-ik_x x)\Big[a_0(x) + \frac{i\eta}{k_z} b_0(x)\Big] = 0 \tag{2.9}$$

$$\exp[i(k_{ix}x' - k_{iz}z')] - \frac{1}{2}\int_{-\infty}^{\infty} dk_x \ \exp[ik_x x' - ik_z z'] \ \left[A_0(k_x) + \frac{i\eta}{k_z} B_0(k_x)\right] = 0 \tag{2.10}$$

Here, $A_0(k_x)$ and $B_0(k_x)$ are the Fourier transform[1] of $a_0(x)$ and $b_0(x)$, respectively. To make above equation independent of x' and z', on taking Fourier transform w.r.t. x' and z', we get

$$\delta(k_x - k_{ix}) - \left[\frac{1}{2}A_0(k_x) + \frac{i\eta}{2k_z} B_0(k_x)\right] = 0 \tag{2.11}$$

Similarly, by Eq. (2.8) we get

$$A_0(k_{1x}) \ = \ \frac{i}{k_{1z}} B_0(k_{1x}) \tag{2.12}$$

On solving Eqs. (2.11) and (2.12) simultaneously, we get

$$A_0(k_x) \ = \ \tilde{A}_0 \delta(k_x - k_{ix}) \tag{2.13}$$

$$B_0(k_x) \ = \ \tilde{B}_0 \delta(k_x - k_{ix}) \tag{2.14}$$

where,

$$\tilde{A}_0 = \frac{2k_{iz}}{k_{iz} + \eta k_{1iz}}$$

and

$$\tilde{B}_0 = \frac{-2ik_{iz}k_{1iz}}{k_{iz} + \eta k_{1iz}}$$

where, k_{1iz} is the $\hat{z}$-component of the propagation constant in lower dielectric medium corresponding to the incident wave. On taking inverse Fourier transform,[2] we get

$$a_0(x) = \tilde{A}_0 \exp(ik_{ix}x) \tag{2.15}$$

$$b_0(x) = \tilde{B}_0 \exp(ik_{ix}x)$$

[1]Fourier transform: $F(k_x) = \frac{1}{2\pi}\int_{-\infty}^{\infty} dx \ \exp(-ik_x x) f(x)$

[2]Inverse Fourier transform: $f(x) = \int_{\infty}^{\infty} dk_x \ \exp(ik_x x) F(k_x)$

For TE Polarisation, $\eta = 1$

$$\tilde{A_0} = \frac{2k_{iz}}{k_{iz} + k_{1iz}} \text{ and } \tilde{B_0} = \frac{-2ik_{iz}k_{1iz}}{k_{iz} + k_{1iz}}$$

For TM Polarisation, $\eta = \frac{\epsilon}{\epsilon_1}$

$$\tilde{A_0} = \frac{2\epsilon_1 k_{iz}}{\epsilon_1 k_{iz} + \epsilon k_{1iz}} \text{ and } \tilde{B_0} = \frac{-2i\epsilon_1 k_{iz}k_{1iz}}{\epsilon_1 k_{iz} + \epsilon k_{1iz}}$$

2.3.2 First order

Assuming small perturbation, we can consider $f(x)$ and $df(x)/dx$, both are of first order. On comparing the first order terms in Eq. (2.7), we get

$$\frac{-1}{2}\int_{-\infty}^{\infty} dk_x \exp(ik_x x' - ik_z z')\ \frac{1}{2\pi}\int_{-\infty}^{\infty} dx\ \exp(-ik_x x)\ (1 + ik_z f(x))\Big[\left(\frac{df(x)}{dx}\frac{k_x}{k_z} + 1\right) (a_0(x) + a_1(x)) + \frac{i\eta}{k_z}(b_0(x) + b_1(x))\Big] = 0 \tag{2.16}$$

$$\frac{-1}{2}\int_{-\infty}^{\infty} dk_x \exp(ik_x x' - ik_z z')\ \frac{1}{2\pi}\int_{-\infty}^{\infty} dx\ \exp(-ik_x x)\Big[\frac{df(x)}{dx}\frac{k_x}{k_z}a_0(x) + a_1(x) + ik_z f(x)a_0(x) + \frac{i\eta}{k_z}(ik_z f(x)b_0(x) + b_1(x))\Big] = 0 \tag{2.17}$$

$$\frac{-1}{2}\int_{-\infty}^{\infty} dk_x \exp(ik_x x' - ik_z z')\Big[\frac{k_x}{k_z}(ik_x F(k_x) * A_0(k_x)) + A_1(k_x) + ik_z(F(k_x) * A_0(k_x)) + \frac{i\eta}{k_z}(B_1(k_x) + ik_z(B_0(k_x) * F(k_x)))\Big] = 0 \tag{2.18}$$

On taking Fourier transform w.r.t. x, we get

$$\frac{k_x}{k_z}(ik_x F(k_x) * A_0(k_x)) + A_1(k_x) + ik_z(F(k_x) * A_0(k_x)) + \frac{i\eta}{k_z}(B_1(k_x) + ik_z(B_0(k_x) * F(k_x))) = 0 \tag{2.19}$$

On substituting $A_0(k_x)$ and $B_0(k_x)$ from Eqs. (2.11) and (2.12), respectively, we get[3]

$$\frac{ik_x}{k_z}(k_x - k_{ix})F(k_x - k_{ix})\tilde{A_0} + A_1(k_x) + ik_z F(k_x - k_{ix})\tilde{A_0} + \frac{i\eta}{k_z}B_1(k_x) - \eta\tilde{B_0}F(k_x - k_{ix}) = 0 \tag{2.20}$$

[3] $F(k_x) * \delta(k_x - k_{ix}) = F(k_x - k_{ix})$

$$-ik_z\tilde{A}_1(k_x) + \eta\tilde{B}_1(k_x) = -k_x(k_x - k_{ix})\tilde{A}_0 - k_z^2\tilde{A}_0 - ik_z\eta\tilde{B}_0 \tag{2.21}$$

Similarly, using Eq. (2.8), we get

$$ik_{1z}\tilde{A}_1(k_x) + \tilde{B}_1(k_x) = -k_{1z}^2\tilde{A}_0 - k_x(k_x - k_{ix})\tilde{A}_0 + ik_{1z}\tilde{B}_0 \tag{2.22}$$

On solving simultaneously, we get

$$A_1(k_x) = \tilde{A}_1(k_x)F(k_x - k_{ix})$$

$$B_1(k_x) = \tilde{B}_1(k_x)F(k_x - k_{ix})$$

where,

$$\tilde{A}_1(k_x) = \frac{-\left(k_z^2 - \eta k_{1z}^2\right)\tilde{A}_0 - k_x(k_x - k_{ix})\left(1-\eta\right)\tilde{A}_0 - i\eta(k_z + k_{1z})\tilde{B}_0}{-ik_z - i\eta k_{1z}}$$

and

$$\tilde{B}_1(k_x) = \frac{ik_zk_{1z}\left(k_z + k_{1z}\right)\tilde{A}_0 + ik_x(k_x - k_{ix})\left(k_z + k_{1z}\right)\tilde{A}_0 + k_zk_{1z}\left(1-\eta\right)\tilde{B}_0}{-ik_z - i\eta k_{1z}}$$

For TE Polarisation, $\eta = 1$

$$\tilde{A}_1(k_x) = i\left(k_{1z} - k_z\right)\tilde{A}_0 + \tilde{B}_0 \text{ and } \tilde{B}_1(k_x) = -k_zk_{1z}\tilde{A}_0 - k_x(k_x - k_{ix})\tilde{A}_0$$

For TM Polarisation, $\eta = \frac{\epsilon}{\epsilon_1}$

$$\tilde{A}_1(k_x) = \frac{-\left(k_z^2 - \frac{\epsilon}{\epsilon_1}k_{1z}^2\right)\tilde{A}_0 - k_x(k_x - k_{ix})\left(1 - \frac{\epsilon}{\epsilon_1}\right)\tilde{A}_0 - i\frac{\epsilon}{\epsilon_1}(k_z + k_{1z})\tilde{B}_0}{-ik_z - i\frac{\epsilon}{\epsilon_1}k_{1z}}$$

and

$$\tilde{B}_1(k_x) = \frac{ik_zk_{1z}\left(k_z + k_{1z}\right)\tilde{A}_0 + ik_x(k_x - k_{ix})\left(k_z + k_{1z}\right)\tilde{A}_0 + k_zk_{1z}\left(1 - \frac{\epsilon}{\epsilon_1}\right)\tilde{B}_0}{-ik_z - i\frac{\epsilon}{\epsilon_1}k_{1z}}$$

2.3.3 Second order

On comparing the coefficient of second order terms we get,

$$\begin{aligned}&\frac{-1}{2}\int_{-\infty}^{\infty} dk_x \exp(ik_xx' - ik_zz')\ \frac{1}{2\pi}\int_{-\infty}^{\infty} dx\ \exp(-ik_xx)\ \Bigg[a_2(x) + \frac{k_x}{k_z}\frac{df(x)}{dx}a_1(x)\\ &+ ik_zf(x)a_1(x) + ik_x\frac{df(x)}{dx}f(x)a_0(x) - \frac{k_z^2}{2}f^2(x)a_0(x) + \frac{i\eta}{k_z}\Big(b_2(x)\\ &+ ik_zf(x)b_1(x) - \frac{k_z^2}{2}f^2(x)b_0(x)\Big)\Bigg] = 0\end{aligned} \tag{2.23}$$

$$A_2(k_x) + \frac{k_x}{k_z}(ik_xF(k_x) * A_1(k_x)) + ik_z(F(k_x) * A_1(k_x)) + ik_x(ik_xF(k_x) * F(k_x) * A_0(k_x))$$
$$- \frac{k_z^2}{2}(F(k_x) * F(k_x) * A_0(k_x)) + \frac{i\eta}{k_z}B_2(k_x) - \eta(F(k_x) * B_1(k_x))$$
$$- \frac{i\eta k_z}{2}(F(k_x) * F(k_x) * B_0(k_x)) = 0 \tag{2.24}$$

On taking ensemble average, we get

$$\langle A_2(k_x)\rangle + \frac{k_x}{k_z}\langle ik_xF(k_x) * A_1(k_x)\rangle + ik_z\langle F(k_x) * A_1(k_x)\rangle + ik_x\langle ik_xF(k_x) * F(k_x) * A_0(k_x)\rangle$$
$$- \frac{k_z^2}{2}\langle F(k_x) * F(k_x) * A_0(k_x)\rangle + \frac{i\eta}{k_z}\langle B_2(k_x)\rangle - \eta\langle F(k_x) * B_1(k_x)\rangle$$
$$- \frac{i\eta k_z}{2}\langle F(k_x) * F(k_x) * B_0(k_x)\rangle = 0 \tag{2.25}$$

$$- ik_{iz}\tilde{A}_2 + \eta\tilde{B}_2 = -i\frac{k_{iz}^3}{2}\tilde{A}_0\int_{-\infty}^{\infty}dk_xW(k_x - k_{ix}) - ik_{ix}k_{iz}\tilde{A}_0\int_{-\infty}^{\infty}dk_xW(k_x - k_{ix})(k_{ix} - k_x)$$
$$- k_{iz}^2\int_{-\infty}^{\infty}dk_xW(k_x - k_{ix})\tilde{A}_1(k_x) - k_{ix}\int_{-\infty}^{\infty}dk_xW(k_x - k_{ix})(k_{ix} - k_x)\tilde{A}_1(k_x)$$
$$+ \frac{\eta k_{iz}^2}{2}\tilde{B}_0\int_{\infty}^{\infty}dk_xW(k_x - k_{ix}) - ik_{iz}\eta\int_{-\infty}^{\infty}dk_xW(k_x - k_{ix})\tilde{B}_1(k_x) \tag{2.26}$$

Similarly, by equation (2.8) we get

$$ik_{1iz}\tilde{A}_2 + \tilde{B}_2 = i\frac{k_{1iz}^3}{2}\tilde{A}_0\int_{-\infty}^{\infty}dk_xW(k_x - k_{ix}) + ik_{ix}k_{1iz}\tilde{A}_0\int_{-\infty}^{\infty}dk_xW(k_x - k_{ix})(k_{ix} - k_x)$$
$$- k_{1iz}^2\int_{-\infty}^{\infty}dk_xW(k_x - k_{ix})\tilde{A}_1(k_x) - k_{ix}\int_{-\infty}^{\infty}dk_xW(k_x - k_{ix})(k_{ix} - k_x)\tilde{A}_1(k_x)$$
$$+ \frac{k_{1iz}^2}{2}\tilde{B}_0\int_{-\infty}^{\infty}dk_xW(k_x - k_{ix}) + ik_{1iz}\int_{-\infty}^{\infty}dk_xW(k_x - k_{ix})\tilde{B}_1(k_x) \tag{2.27}$$

For TE Polarisation, $\eta = 1$

$$- ik_{iz}\tilde{A}_2 + \tilde{B}_2 = -i\frac{k_{iz}^3}{2}\tilde{A}_0\int_{-\infty}^{\infty}dk_xW(k_x - k_{ix}) - ik_{ix}k_{iz}\tilde{A}_0\int_{-\infty}^{\infty}dk_xW(k_x - k_{ix})(k_{ix} - k_x)$$
$$- k_{iz}^2\int_{-\infty}^{\infty}dk_xW(k_x - k_{ix})\tilde{A}_1(k_x) - k_{ix}\int_{-\infty}^{\infty}dk_xW(k_x - k_{ix})(k_{ix} - k_x)\tilde{A}_1(k_x)$$
$$+ \frac{k_{iz}^2}{2}\tilde{B}_0\int_{\infty}^{\infty}dk_xW(k_x - k_{ix}) - ik_{iz}\int_{-\infty}^{\infty}dk_xW(k_x - k_{ix})\tilde{B}_1(k_x) \tag{2.28}$$

and

$$ik_{1iz}\tilde{A}_2 + \tilde{B}_2 = i\frac{k_{1iz}^3}{2}\tilde{A}_0\int_{-\infty}^{\infty} dk_x W(k_x - k_{ix}) + ik_{ix}k_{1iz}\tilde{A}_0\int_{-\infty}^{\infty} dk_x W(k_x - k_{ix})(k_{ix} - k_x)$$
$$- k_{1iz}^2\int_{-\infty}^{\infty} dk_x W(k_x - k_{ix})\tilde{A}_1(k_x) - k_{ix}\int_{-\infty}^{\infty} dk_x W(k_x - k_{ix})(k_{ix} - k_x)\tilde{A}_1(k_x)$$
$$+ \frac{k_{1iz}^2}{2}\tilde{B}_0\int_{-\infty}^{\infty} dk_x W(k_x - k_{ix}) + ik_{1iz}\int_{-\infty}^{\infty} dk_x W(k_x - k_{ix})\tilde{B}_1(k_x) \tag{2.29}$$

By Eqs.(2.28) and (2.29), we get

$$\begin{aligned}\tilde{A}_2 = \frac{h^2}{2}\tilde{A}_0(k_{iz}^2 + k_{1iz}^2 - k_{iz}k_{1iz}) + i(k_{1iz} - k_{iz})\int_{-\infty}^{\infty} dk_x\tilde{A}_1(k_x)W(k_x - k_{ix}) \\ + i\frac{k_{iz} - k_{1iz}}{2}h^2\tilde{B}_0 + \int_{-\infty}^{\infty} dk_x\tilde{B}_1(k_x)W(k_x - k_{ix})\end{aligned} \tag{2.30}$$

and

$$\begin{aligned}\tilde{B}_2 = ik_{iz}(k_{1iz}^2 - k_{iz}k_{1iz})\frac{h^2}{2}\tilde{A}_0 - k_{iz}k_{1iz}\int_{-\infty}^{\infty} dk_x\tilde{A}_1(k_x)W(k_x - k_{ix}) \\ + k_{iz}k_{1iz}\frac{h^2}{2}\tilde{B}_0 - k_{ix}\int_{-\infty}^{\infty} dk_x W(k_x - k_{ix})(k_{ix} - k_x)\tilde{A}_1(k_x)\end{aligned} \tag{2.31}$$

For TM Polarisation, $\eta = \frac{\epsilon}{\epsilon_1}$

$$-ik_{iz}\tilde{A}_2 + \frac{\epsilon}{\epsilon_1}\tilde{B}_2 = -i\frac{k_{iz}^3}{2}\tilde{A}_0\int_{-\infty}^{\infty} dk_x W(k_x - k_{ix}) - ik_{ix}k_{iz}\tilde{A}_0\int_{-\infty}^{\infty} dk_x W(k_x - k_{ix})(k_{ix} - k_x)$$
$$- k_{iz}^2\int_{-\infty}^{\infty} dk_x W(k_x - k_{ix})\tilde{A}_1(k_x) - k_{ix}\int_{-\infty}^{\infty} dk_x W(k_x - k_{ix})(k_{ix} - k_x)\tilde{A}_1(k_x)$$
$$+ \frac{\epsilon k_{iz}^2}{2\epsilon_1}\tilde{B}_0\int_{\infty}^{\infty} dk_x W(k_x - k_{ix}) - ik_{iz}\frac{\epsilon}{\epsilon_1}\int_{-\infty}^{\infty} dk_x W(k_x - k_{ix})\tilde{B}_1(k_x) \tag{2.32}$$

and

$$ik_{1iz}\tilde{A}_2 + \tilde{B}_2 = i\frac{k_{1iz}^3}{2}\tilde{A}_0\int_{-\infty}^{\infty} dk_x W(k_x - k_{ix}) + ik_{ix}k_{1iz}\tilde{A}_0\int_{-\infty}^{\infty} dk_x W(k_x - k_{ix})(k_{ix} - k_x)$$
$$- k_{1iz}^2\int_{-\infty}^{\infty} dk_x W(k_x - k_{ix})\tilde{A}_1(k_x) - k_{ix}\int_{-\infty}^{\infty} dk_x W(k_x - k_{ix})(k_{ix} - k_x)\tilde{A}_1(k_x)$$
$$+ \frac{k_{1iz}^2}{2}\tilde{B}_0\int_{-\infty}^{\infty} dk_x W(k_x - k_{ix}) + ik_{1iz}\int_{-\infty}^{\infty} dk_x W(k_x - k_{ix})\tilde{B}_1(k_x) \tag{2.33}$$

In this chapter, we have determined the expressions for surface field unknowns, $a(x)$ and $b(x)$ up to second order terms for both TE and TM polarisations. In the next chapter, we will continue the analysis for determining the scattered field expressions for both TE and TM polarisations.

Chapter 3

Scattered Field from Random Rough Surfaces

In the last chapter, we derived the expressions for different orders of surface field unknowns. In this chapter, we derived the expressions for the scattered field for zeroth, first and second orders of perturbation in random rough surface profile, $f(x)$.

3.1 Scattered Field

According to extinction theorem, the total field in a medium is defined as the superposition of the field due to the source in that medium and the field due to the surface sources at the interface. In our problem statement, their is no field source in lower dielectric medium. So, the field in medium 1 due to the surface source at the interface will be the scattered field. Hence, the scattered field, ψ_s, is given by

$$\psi_s = \int_s dx \left[a(x)\sqrt{1+\left(\frac{df}{dx}\right)^2}\,\hat{n}\cdot\nabla g(\overrightarrow{r},\overrightarrow{r}') - g(\overrightarrow{r},\overrightarrow{r}')\,\eta\,b(x)\right], \text{ for } z' > f(x) \tag{3.1}$$

On substituting expressions for $a(x)$, $b(x)$ and Green's function, we get

$$\psi_s = -\frac{1}{2}\int_{-\infty}^{\infty} dk_x \left[\exp(ik_x x' + ik_z z')\,\frac{1}{2\pi}\int_{-\infty}^{\infty} dx \exp(-ik_x x - ik_z f(x))\left[\left(\frac{df(x)}{dx}\frac{k_x}{k_z} - 1\right)(a_0(x)+a_1(x)+a_2(x)+\cdots) + \frac{i\eta}{k_z}(b_0(x)+b_1(x)+b_2(x)+\cdots)\right]\right] \tag{3.2}$$

Now we evaluate the different order terms individually.

3.1.1 Zeroth Order

The terms in which the degree of $f(x)$, of derivative of $f(x)$ or of their combination is zero are known as zeroth order terms. Here, we are assuming that the random rough

surface profile, $f(x)$, is a slowly varying function, which provides us the freedom to assume order of $f(x)$ and its derivative as same. On comparing the zeroth order terms of Eq. (3.2), the zeroth order scattered field ψ_{s0} will be given by

$$\psi_{s0} = -\frac{1}{2}\int_{-\infty}^{\infty} dk_x \left[\exp(ik_x x' + ik_z z') \frac{1}{2\pi}\int_{-\infty}^{\infty} dx \exp(-ik_x x)\left[-a_0(x) + \frac{i\eta}{k_z} b_0(x)\right]\right] \tag{3.3}$$

$$= -\frac{1}{2}\int_{-\infty}^{\infty} dk_x \left[\exp(ik_x x' + ik_z z') \left[-A_0(k_x) + \frac{i\eta}{k_z} B_0(k_x)\right]\right] \tag{3.4}$$

On substituting expressions for $A_0(k_x)$ and $B_0(k_x)$ and simplifying, we get

$$\psi_{s0}(k_x) = \tilde{\psi}_{s0}\delta(k_x - k_{ix}) \tag{3.5}$$

or

$$\psi_{s0}(x', z') = \tilde{\psi}_{s0} \exp(ik_{ix}x' + ik_{iz}z') \tag{3.6}$$

where,

$$\tilde{\psi}_{s0} = \frac{k_{iz} - \eta\ k_{1iz}}{k_{iz} + \eta\ k_{1iz}} \tag{3.7}$$

For TE Polarisation, $\eta = 1$

$$\tilde{\psi}_{s0} = \frac{k_{iz} - k_{1iz}}{k_{iz} + k_{1iz}} \tag{3.8}$$

For TM polarisation, $\eta = \frac{\epsilon}{\epsilon_1}$

$$\tilde{\psi}_{s0} = \frac{\epsilon_1 k_{iz} - \epsilon k_{1iz}}{\epsilon_1 k_{iz} + \epsilon k_{1iz}} \tag{3.9}$$

3.1.2 First Order

The terms in which the degree of $f(x)$, of derivative of $f(x)$ or of their combination is one are known as first order terms. On comparing the first order terms of Eq. (3.2), the first order scattered field, ψ_{s1} is given by

$$\psi_{s1} = -\frac{1}{2}\int_{-\infty}^{\infty} dk_x \Big[\exp(ik_x x' + ik_z z') \frac{1}{2\pi}\int_{-\infty}^{\infty} dx \exp(-ik_x x)\Big[\frac{df(x)}{dx}\frac{k_x}{k_z}a_0(x) - a_1(x) + ik_z f(x)a_0(x) + \frac{i\eta}{k_z}(-ik_z f(x)b_0(x) + b_1(x))\Big]\Big] \tag{3.10}$$

$$= -\frac{1}{2}\int_{-\infty}^{\infty} dk_x \ \exp(ik_x x' + ik_z z') \ \Big[i\frac{k_x}{k_z}\tilde{A}_0(k_x - k_{ix})F(k_x - k_{ix}) - \tilde{A}_1(k_x)F(k_x - k_{ix}) + ik_z\tilde{A}_0 F(k_x - k_{ix}) + \eta\tilde{B}_0 F(k_x - k_{ix}) + \frac{i\eta}{k_z}\tilde{B}_1(k_x)F(k_x - k_{ix})\Big] \tag{3.11}$$

On taking Fourier transform, we get

$$\psi_{s1}(k_x) = \tilde{\psi}_{s1}(k_x)F(k_x - k_{ix}) \tag{3.12}$$

where,

$$\tilde{\psi}_{s1} = \frac{i}{2k_z}\Big[-k_z^2\tilde{A}_0 - k_x(k_x - k_{ix})\tilde{A}_0 - ik_z\tilde{A}_1(k_x) + ik_z\eta\tilde{B}_0 - \eta\tilde{B}_1(k_x)\Big] \tag{3.13}$$

On substituting expressions of $\tilde{A}_0$, $\tilde{B}_0$, $\tilde{A}_1(k_x)$ and $\tilde{B}_1(k_x)$ in above equation and simplification, we get

$$\tilde{\psi}_{s1} = \frac{2ik_{iz}\left[(\eta - 1)(\eta k_{1iz}k_{1z} - k_x(k_{ix} - k_x)) + \eta k_{1z}^2 - k_z^2\right]}{(k_{iz} + \eta k_{1iz})(k_z + \eta k_{1z})} \tag{3.14}$$

For TE Polarisation, $\eta = 1$

$$\tilde{\psi}_{s1} = \frac{2ik_{iz}(k_{1z} - k_z)}{k_{iz} + k_{1iz}} \tag{3.15}$$

For TM Polarisation, $\eta = \frac{\epsilon}{\epsilon_1}$

$$\tilde{\psi}_{s1} = \frac{-2ik_{iz}\epsilon_1\left[k_z^2 - \frac{\epsilon}{\epsilon_1}k_{1z}^2 + \left(1 - \frac{\epsilon}{\epsilon_1}\right)(k_x^2 - k_x k_{ix})\right] - i\epsilon(1 - \frac{\epsilon}{\epsilon_1})k_{iz}k_{1z}k_{1iz}}{k_z(\epsilon_1 k_{iz} + \epsilon k_{1iz}) + \epsilon k_{1z}\left(k_{iz} + \frac{\epsilon}{\epsilon_1}k_{1iz}\right)} \tag{3.16}$$

3.1.3 Second Order

The terms in which the degree of $f(x)$, of derivative of $f(x)$ or of their combination is two are known as second order terms. On comparing the second order terms of Eq. (3.2), the second order scattered field, ψ_{s2} is given by

$$\psi_{s2}(x') = -\frac{1}{2}\int_{-\infty}^{\infty} dk_x \ \exp(ik_x x' + ik_z z') \ \frac{1}{2\pi}\int_{-\infty}^{\infty} dx \ \exp(-ik_x x) \ [-a_2(x) + \frac{k_x}{k_z}\frac{df(x)}{dx}a_1(x) + ik_z f(x)a_1(x) - ik_x f(x)\frac{df(x)}{dx}a_0(x) + \frac{k_z^2}{2}f^2(x)a_0(x) + \frac{i\eta}{k_z}b_2(x) + \eta f(x)b_1(x) - i\frac{\eta k_z}{2}f^2(x)b_0(x)] \tag{3.17}$$

On solving the inner integral, we get

$$\begin{aligned}\psi_{s2}(x') = -\frac{1}{2}\int_{-\infty}^{\infty} dk_x \exp(ik_x x' + ik_z z')\Big(- A_2(k_x) + \frac{k_x}{k_z}(ik_x F(k_x) * A_1(k_x)) \\ + ik_z(F(k_x) * A_1(k_x)) - ik_x(ik_x F(k_x) * F(k_x) * A_0(k_x)) \\ + \frac{k_z^2}{2}(F(k_x) * F(k_x) * A_0(k_x)) + \eta(F(k_x) * B_1(k_x)) \\ - i\frac{\eta k_z}{2}(F(k_x) * F(k_x) * B_0(k_x)) + \frac{i\eta}{k_z}B_2(k_x)\Big)\end{aligned} \tag{3.18}$$

On taking Fourier transform w.r.t. x', we get

$$\begin{aligned}\psi_{s2}(k_x) = -\frac{1}{2}\Big(- A_2(k_x) + \frac{k_x}{k_z}(ik_x F(k_x) * A_1(k_x)) + ik_z(F(k_x) * A_1(k_x)) \\ - ik_x(ik_x F(k_x) * F(k_x) * A_0(k_x)) + \frac{k_z^2}{2}(F(k_x) * F(k_x) * A_0(k_x)) \\ + \eta(F(k_x) * B_1(k_x)) - i\frac{\eta k_z}{2}(F(k_x) * F(k_x) * B_0(k_x)) + \frac{i\eta}{k_z}B_2(k_x)\Big)\end{aligned} \tag{3.19}$$

On taking ensemble average of the above equation, we get

$$\begin{aligned}\langle\psi_{s2}(k_x)\rangle = \Big[\frac{\tilde{A}_2}{2} - i\frac{k_{ix}}{2k_{iz}}\int_{-\infty}^{\infty} dk_x\ (k_{ix} - k_x)\tilde{A}_1(k_x)W(k_x - k_{ix}) \\ - i\frac{k_{iz}}{2}\int_{-\infty}^{\infty} dk_x\ \tilde{A}_1(k_x)W(k_x - k_{ix}) - \frac{k_{ix}}{2}\tilde{A}_0\int_{-\infty}^{\infty} dk_x\ (k_{ix} - k_x)W(k_x - k_{ix}) \\ - \frac{k_{iz}^2}{4}\tilde{A}_0\int_{-\infty}^{\infty} dk_x\ W(k_x - k_{ix}) - i\frac{\eta}{2k_{iz}}\tilde{B}_2 - \frac{\eta}{2}\int_{-\infty}^{\infty} dk_x\ \tilde{B}_1(k_x)W(k_x - k_{ix}) \\ + i\frac{\eta k_{iz}}{4}\tilde{B}_0\int_{-\infty}^{\infty} dk_x\ W(k_x - k_{ix})\Big]\delta(k_x - k_{ix})\end{aligned} \tag{3.20}$$

On substituting expressions for $A_1(k_x)$, $B_1(k_x)$, $A_0(k_x)$ and $B_0(k_x)$ and simplification, we get

$$\langle\psi_{s2}(k_x)\rangle = \tilde{\psi}_{s2}\delta(k_x - k_{ix}) \tag{3.21}$$

where,

$$\begin{aligned}\tilde{\psi}_{s2} = -\frac{k_{iz}^2 h^2}{2}\tilde{\psi}_{s0} + \frac{\tilde{A}_2}{2} - i\frac{\eta}{2k_{iz}}\tilde{B}_2 - i\frac{k_{ix}}{2k_{iz}}\int_{-\infty}^{\infty} dk_x\ (k_{ix} - k_x)\tilde{A}_1(k_x)W(k_x - k_{ix}) \\ - i\frac{k_{iz}}{2}\int_{-\infty}^{\infty} dk_x\ \tilde{A}_1(k_x)W(k_x - k_{ix}) - \frac{\eta}{2}\int_{-\infty}^{\infty} dk_x\ \tilde{B}_1(k_x)W(k_x - k_{ix})\end{aligned} \tag{3.22}$$

For TE Polarisation, $\eta = 1$

$$\begin{aligned}\tilde{\psi}_{s2} = &-\frac{k_{iz}^2 h^2}{2}\tilde{\psi}_{s0} + \frac{\tilde{A}_2}{2} - i\frac{k_{ix}}{2k_{iz}}\int_{-\infty}^{\infty} dk_x\ (k_{ix}-k_x)\tilde{A}_1(k_x)W(k_x-k_{ix}) \\ &- i\frac{k_{iz}}{2}\int_{-\infty}^{\infty} dk_x\ \tilde{A}_1(k_x)W(k_x-k_{ix}) - i\frac{1}{2k_{iz}}\tilde{B}_2 \\ &- \frac{1}{2}\int_{-\infty}^{\infty} dk_x\ \tilde{B}_1(k_x)W(k_x-k_{ix}) \end{aligned} \tag{3.23}$$

$$\tilde{\psi}_{s2} = -2k_{iz}k_{1iz}h^2\tilde{\psi}_{s0} + 2k_{iz}\tilde{\psi}_{s0}\int_{-\infty}^{\infty} dk_x(k_{1z}-k_z)W(k_x-k_{ix}) \tag{3.24}$$

For TM Polarisation, $\eta = \frac{\epsilon}{\epsilon_1}$

$$\begin{aligned}\tilde{\psi}_{s2} = &-\frac{k_{iz}^2 h^2}{2}\tilde{\psi}_{s0} + \frac{\tilde{A}_2}{2} - i\frac{\epsilon}{2\epsilon_1 k_{iz}}\tilde{B}_2 - i\frac{k_{ix}}{2k_{iz}}\int_{-\infty}^{\infty} dk_x\ (k_{ix}-k_x)\tilde{A}_1(k_x)W(k_x-k_{ix}) \\ &- i\frac{k_{iz}}{2}\int_{-\infty}^{\infty} dk_x\ \tilde{A}_1(k_x)W(k_x-k_{ix}) - \frac{\epsilon}{2\epsilon_1}\int_{-\infty}^{\infty} dk_x\ \tilde{B}_1(k_x)W(k_x-k_{ix}) \end{aligned} \tag{3.25}$$

3.2 Scattered Field as a Function of Incident and Scattered Angles

In the last section, we derived the expressions for the zeroth, first and second order scattered fields. In this section, we transform them as a function of incident angle, θ_i, and scattered angle, θ_s, which is more convenient form for analysis and visualisation. From the Fig. 3.1, we get

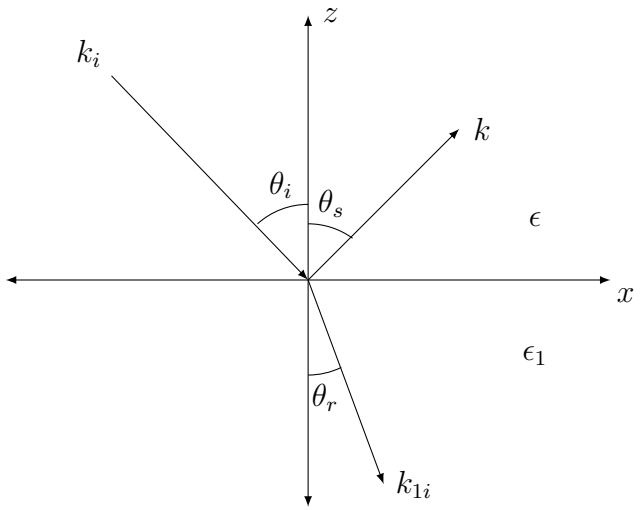

Figure 3.1: Decomposition of propagation vectors along x- and z-axes

$$\begin{aligned} k_{ix} &= k_{1ix} \\ &= k\sin\theta_i \\ k_{iz} &= -k\cos\theta_i \\ k_{1iz} &= -k\sqrt{\epsilon_r - \sin^2\theta_i} \\ k_x &= k\sin\theta_s \\ k_z &= -k\ \cos\theta_s \\ k_{1iz} &= -k\sqrt{\epsilon_r - \sin^2\theta_s} \end{aligned} \tag{3.26}$$

where k is the propagation constant in upper dielectric medium, θ_i and θ_s be the incident and scattering angle w.r.t. normal to the surface, respectively, as shown in Fig. 3.1, and ϵ_r be the the relative electrical permittivity of the lower dielectric medium w.r.t. upper dielectric medium.

3.2.1 Zeroth Order

On substituting Eq (3.26) in Eq (3.7) and simplification, we get

$$\psi_{s0}(\theta_i,\theta_s) = \frac{\cos\theta_i - \eta\sqrt{\epsilon_r - \sin^2\theta_i}}{\cos\theta_i + \eta\sqrt{\epsilon_r - \sin^2\theta_i}}\ \delta(k[\sin\theta_s - \sin\theta_i]) \tag{3.27}$$

and the corresponding scattered power is given by the mod square of the scattered field. On taking mod square of the above equation, we get

$$|\psi_{s0}(\theta_i,\theta_s)|^2 = \frac{(1+\eta^2)\cos^2\theta_i + \eta^2(\epsilon_r - 1) - 2\eta\cos\theta_i\sqrt{\epsilon_r - \sin^2\theta_i}}{(1+\eta^2)\cos^2\theta_i + \eta^2(\epsilon_r - 1) + 2\eta\cos\theta_i\sqrt{\epsilon_r - \sin^2\theta_i}} \delta(k[\sin\theta_s - \sin\theta_i]) \tag{3.28}$$

For TE Polarisation, $\eta = 1$

$$\psi_{s0}(\theta_i,\theta_s) = \frac{\cos\theta_i - \sqrt{\epsilon_r - \sin^2\theta_i}}{\cos\theta_i + \sqrt{\epsilon_r - \sin^2\theta_i}}\ \delta(k[\sin\theta_s - \sin\theta_i]) \tag{3.29}$$

and

$$|\psi_{s0}(\theta_i,\theta_s)|^2 = \frac{\cos 2\theta_i + \epsilon_r - 2\cos\theta_i\sqrt{\epsilon_r - \sin^2\theta_i}}{\cos 2\theta_i + \epsilon_r + 2\cos\theta_i\sqrt{\epsilon_r - \sin^2\theta_i}}\ \delta(k[\sin\theta_s - \sin\theta_i]) \tag{3.30}$$

The variation of the zeroth order reflected power in specular direction for an TE polarised incident field as a function of the incident angle is shown in Fig. 3.2. Typical Parameter: relative electrical permittivity, $\epsilon_r = 3$.

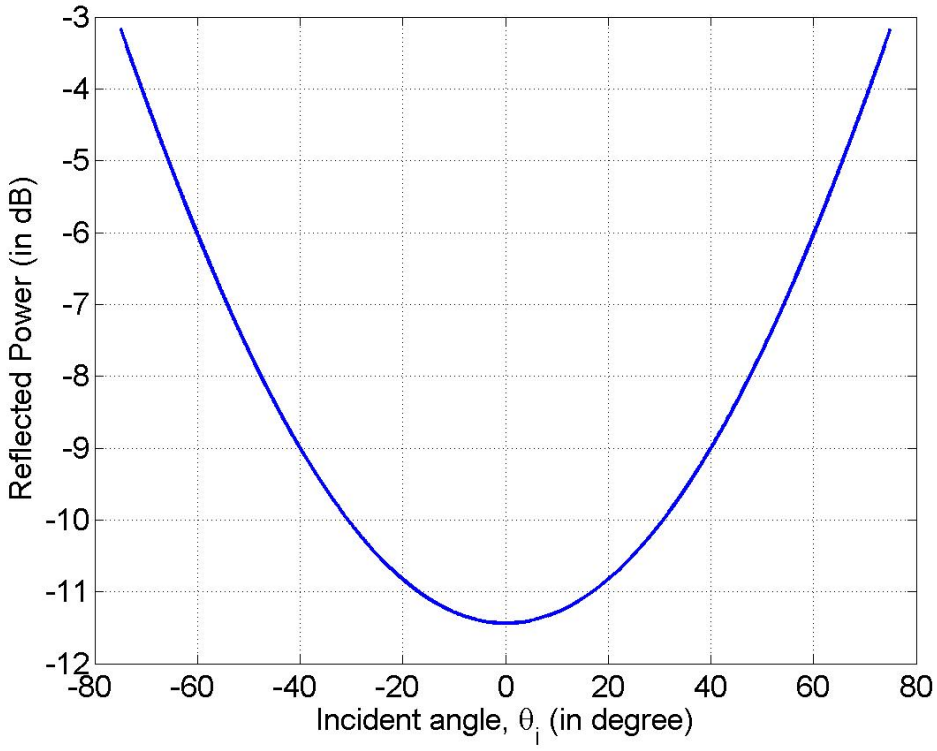

Figure 3.2: Zeroth order Reflected power in specular direction for TE polarisation as a function of the incident angle, θ_i

For TM Polarisation, $\eta = \frac{\epsilon}{\epsilon_1}$

$$\psi_{s0}(\theta_i, \theta_s) = \frac{\epsilon_r \cos\theta_i - \sqrt{\epsilon_r - \sin^2\theta_i}}{\epsilon_r \cos\theta_i + \sqrt{\epsilon_r - \sin^2\theta_i}} \; \delta(k[\sin\theta_s - \sin\theta_i]) \tag{3.31}$$

and

$$|\psi_{s0}(\theta_i, \theta_s)|^2 = \frac{(\epsilon_r^2 + 1)\cos^2\theta_i + (\epsilon_r - 1) - 2\epsilon_r \cos\theta_i \sqrt{\epsilon_r - \sin^2\theta_i}}{(\epsilon_r^2 + 1)\cos^2\theta_i + (\epsilon_r - 1) + 2\epsilon_r \cos\theta_i \sqrt{\epsilon_r - \sin^2\theta_i}} \; \delta(k[\sin\theta_s - \sin\theta_i]) \tag{3.32}$$

The variation of the zeroth order reflected power in specular direction for an TM polarised incident field as a function of the incident angle is shown in Fig. 3.3. Typical Parameter: relative electrical permittivity, $\epsilon_r = 3$.

3.2.2 First Order

On substituting Eq (3.26) in Eq (3.14) and simplification, we get

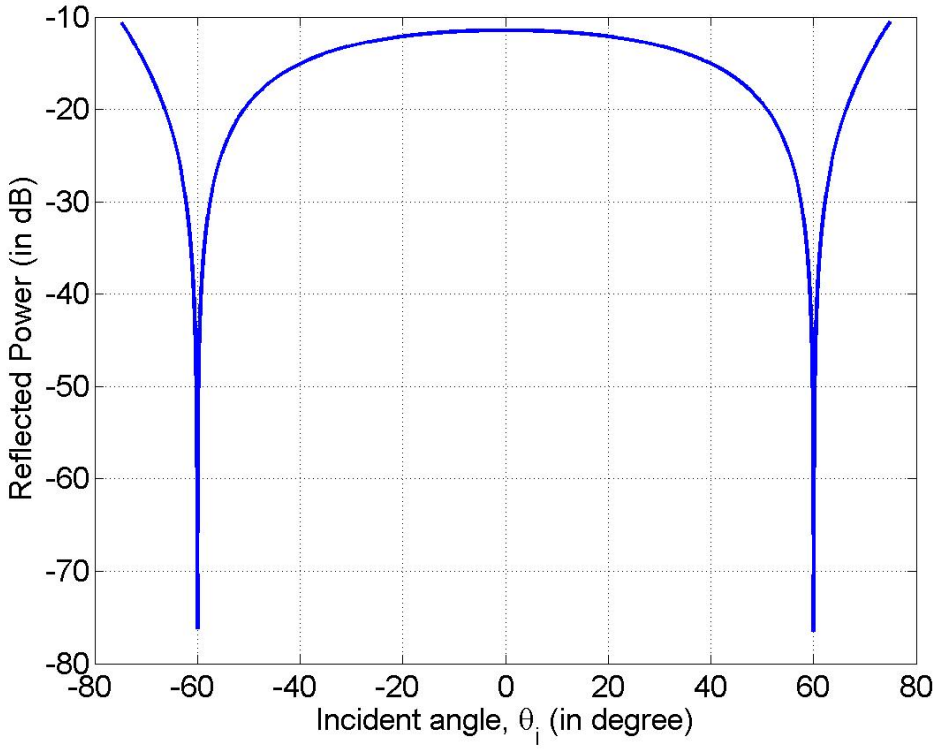

Figure 3.3: Zeroth order reflected power in specular direction for TM polarisation as a function of the incident angle, θ_i

$$\psi_{s1}(\theta_i,\theta_s) = \frac{-2ik\cos\theta_i\left[(\eta-1)(\eta\sqrt{\epsilon_r-\sin^2\theta_i}\sqrt{\epsilon_r-\sin^2\theta_i}-\sin\theta_s(\sin\theta_i-\sin\theta_s))\right]}{(\cos\theta_s+\eta\sqrt{\epsilon_r-\sin^2\theta_s})(\cos\theta_i+\eta\sqrt{\epsilon_r-\sin^2\theta_i})} F(k[\sin\theta_s-\sin\theta_i]) \tag{3.33}$$

For TE Polarisation, $\eta = 1$

$$\psi_{s1}(\theta_i,\theta_s) = \frac{-2ik\cos\theta_i\,(\epsilon_r-1)}{(\cos\theta_s+\sqrt{\epsilon_r-\sin^2\theta_s})(\cos\theta_i+\sqrt{\epsilon_r-\sin^2\theta_i})} F(k[\sin\theta_s-\sin\theta_i]) \tag{3.34}$$

and the corresponding ensemble averaged scattered power will be given by

$$\langle|\psi_{s1}(\theta_i,\theta_s)|^2\rangle = \left|\frac{-2k\cos\theta_i\,(\epsilon_r-1)}{(\cos\theta_s+\sqrt{\epsilon_r-\sin^2\theta_s})(\cos\theta_i+\sqrt{\epsilon_r-\sin^2\theta_i})}\right|^2 W(k[\sin\theta_s-\sin\theta_i]) \tag{3.35}$$

The variation in scattered power as a function of the scattering angle for TE polarised field incident at 40° w.r.t. the normal to the surface is shown in Fig. 3.4 and 3.5.

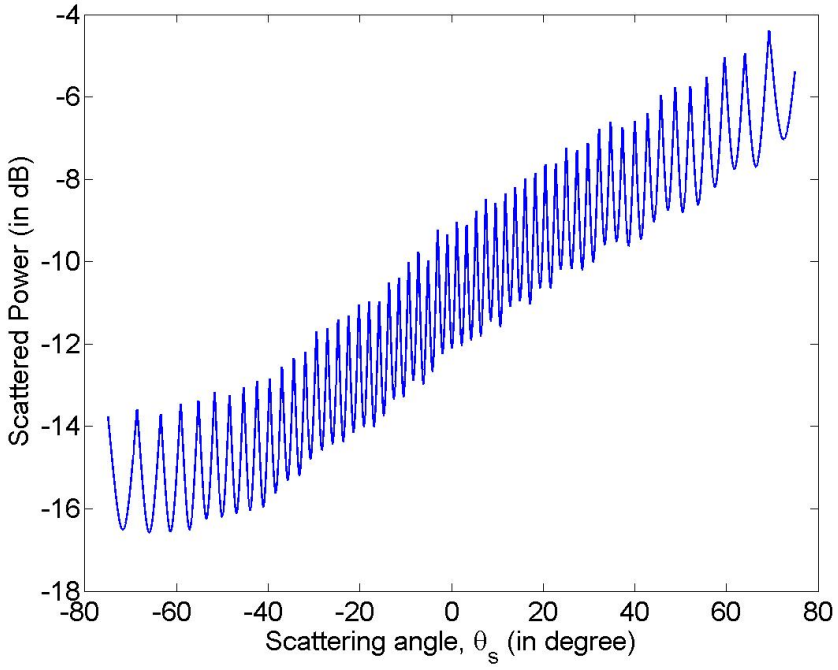

Figure 3.4: First order scattered power for TE polarisation as a function of the scattering angle, θ_s at incident angle, $\theta_i = 40°$ ensemble averaged over 1000 surfaces.

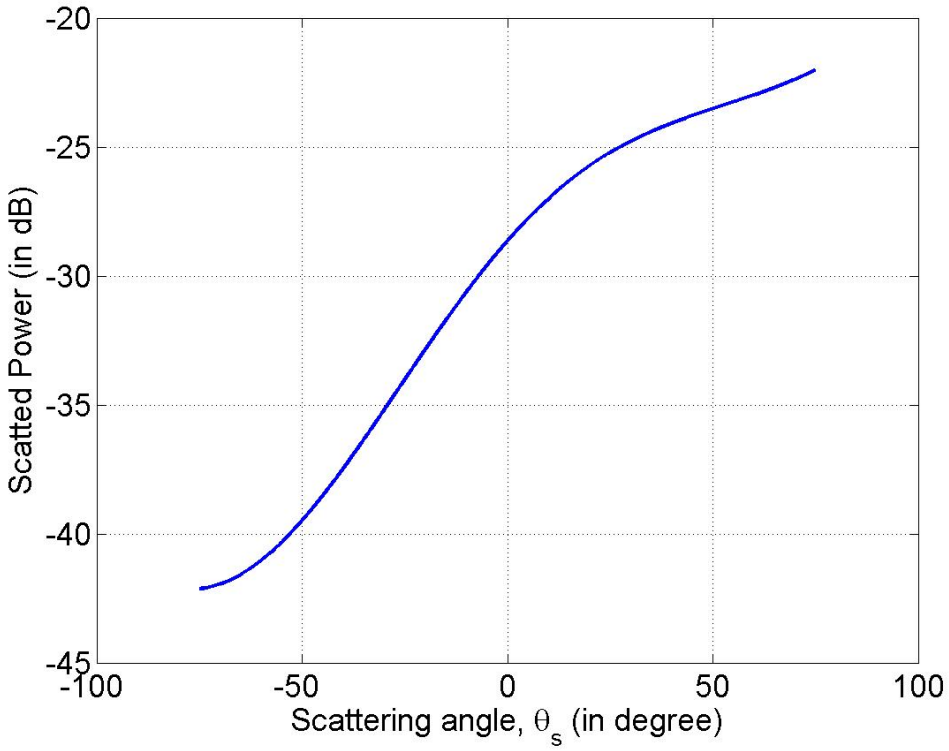

Figure 3.5: First order scattered power for TE polarisation as a function of the scattering angle, θ_s at incident angle, $\theta_i = 40°$.

Fig. 3.4 is plotted by using Eq (3.34) and random rough surface generated using the method given by Thorsos [6] and ensemble averaged over 1000 surfaces. Whereas, Fig. 3.35 is plotted using the Eq (3.35). Typical Parameters used are: wavelength, $\lambda = 23cm$, incident angle, $\theta_i = 40^\circ$, relative electrical permittivity, $\epsilon_r = 3$ and Gaussian auto correlation function with rms height, $h = 1cm$ and surface correlation length, $l = 10cm$, surface length, $L = 9.2m$.

For TM Polarisation, $\eta = \frac{\epsilon}{\epsilon_1}$

$$\psi_{s1}(\theta_i, \theta_s) = \frac{-2ik(\epsilon_r - 1)\cos\theta_i \left[\epsilon_r \sin\theta_i \sin\theta_s - \sqrt{\epsilon_r - \sin^2\theta_i}\sqrt{\epsilon_r - \sin^2\theta_s}\right]}{\left(\epsilon_r \cos\theta_i + \sqrt{\epsilon_r - \sin^2\theta_i}\right)\left(\epsilon_r \cos\theta_s + \sqrt{\epsilon_r - \sin^2\theta_s}\right)} F(k[\sin\theta_s - \sin\theta_i]) \quad (3.36)$$

and the corresponding ensemble averaged scattered power will be given by

$$\langle|\psi_{s1}|^2\rangle = \left|\frac{-2k(\epsilon_r - 1)\cos\theta_i \left[\epsilon_r \sin\theta_i \sin\theta_s - \sqrt{\epsilon_r - \sin^2\theta_i}\sqrt{\epsilon_r - \sin^2\theta_s}\right]}{\left(\epsilon_r \cos\theta_i + \sqrt{\epsilon_r - \sin^2\theta_i}\right)\left(\epsilon_r \cos\theta_s + \sqrt{\epsilon_r - \sin^2\theta_s}\right)}\right|^2 W(k[\sin\theta_s - \sin\theta_i]) \quad (3.37)$$

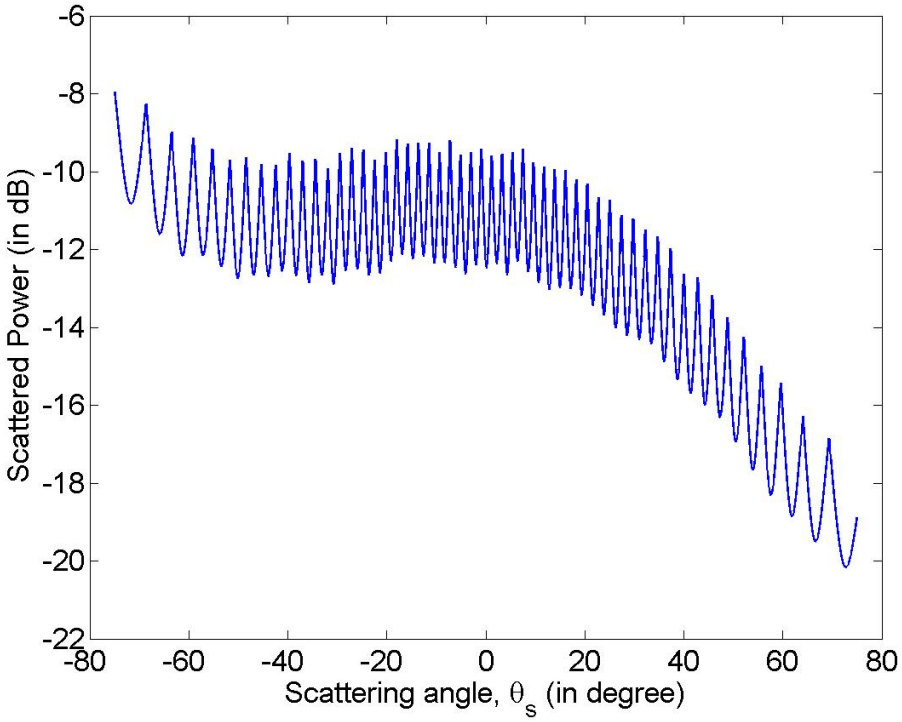

Figure 3.6: First order scattered power for TM polarisation as a function of the scattering angle, θ_s at incident angle, $\theta_i = 40^\circ$ ensemble averaged over 1000 surfaces.

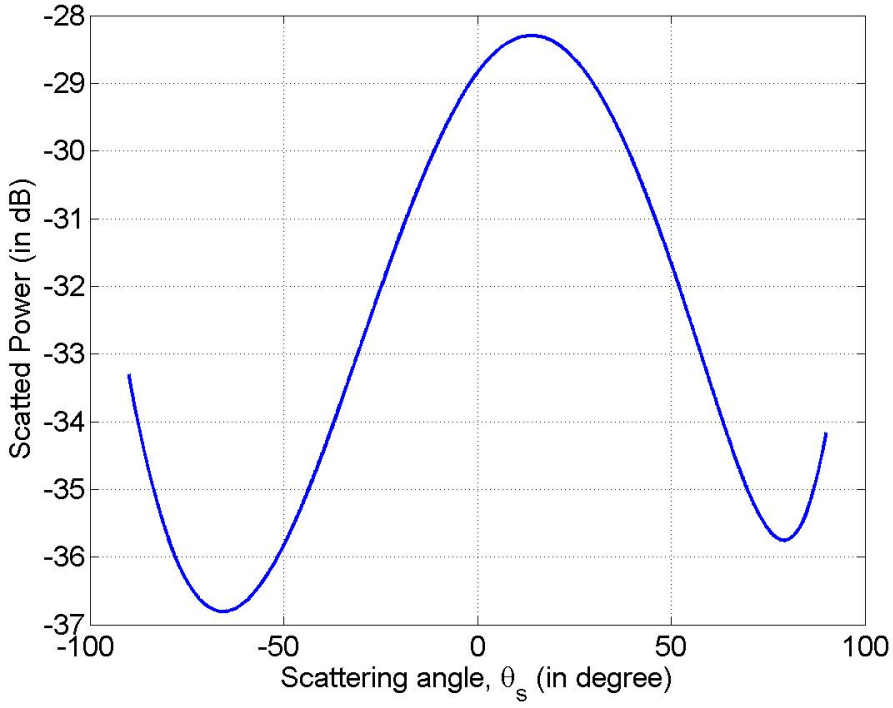

Figure 3.7: First order scattered power for TM polarisation as a function of the scattering angle, θ_s at incident angle, $\theta_i = 40°$.

The variation in scattered power as a function of the scattering angle for TM polarised field incident at 40° w.r.t. normal to the surface is shown in Fig. 3.6 and 3.7.

Fig. 3.6 is plotted by using Eq (3.36) and random rough surface generated using the method given by Thorsos [6] and ensemble averaged over 1000 surfaces. Whereas, Fig. 3.37 is plotted using the Eq (3.35). Typical Parameters used are: wavelength, $\lambda = 23cm$, incident angle, $\theta_i = 40°$, relative electrical permittivity, $\epsilon_r = 3$ and Gaussian auto correlation function with rms height, $h = 1cm$ and surface correlation length, $l = 10cm$, surface length, $L = 9.2m$.

In summary, we have derived the scattered field expressions for the zeroth, first and second orders of random rough surface profile, $f(x)$ in this chapter. In the next Chapter, we will use these expressions and compare the two types of icy surfaces: random rough surface and random rough surface with uniformly distributed smooth square boulders, on the basis of RCS (Radar Cross Section) and CPR (Circular Polarisation Ratio).

Chapter 4

Ice Configurations: Analysis using RCS and CPR

In the previous chapters, we analysed the electromagnetic wave scattering from random rough surfaces for both TE (Transverse Electric) and TM (Transverse Magnetic) polarisations. In the analysis, we observed that scattering behaviour were different for TE and TM polarisations. Which means, surface will behave differently for $\hat{h}$- and $\hat{v}$-pol (Horizontal and Vertical Polarisation, respectively). It means that if we transmit a circularly polarised signal, then the reflected field may be an elliptically polarised signal, due to the different reflection co-efficients for horizontal and vertical components. By the principle of orthogonality, we can decompose it into RHCP (Right Handed Circularly Polarised) and LHCP (Left Handed Circularly Polarised) signals. In this chapter, we analyse the two types of icy surface configurations: random rough surface and random rough surface with uniformly distributed smooth square boulders, on the basis of RCS (Radar Cross Section) and CPR (Circular Polarisation Ratio).

4.1 Radar Cross Section (RCS)

Radar cross section (RCS) is defined as the ratio of the backscattered power per unit steradian to the total incident power on the target. RCS is basically same as commonly used term reflection co-efficient and is a good measure to calculate how much a target reflect power in the direction of the receiver.

Considering up to second order terms, the total scattered field is given by

$$\psi_s = \psi_{s0} + \psi_{s1} + \psi_{s2} \tag{4.1}$$

and the corresponding scattered power is given by the mod square of the scattered field, which is equal to the product of field and its complex conjugate.

$$|\psi_s|^2 = \psi_s \psi_s^* \tag{4.2}$$

$$= (\psi_{s0} + \psi_{s1} + \psi_{s2})\ (\psi_{s0} + \psi_{s1} + \psi_{s2})^* \tag{4.3}$$

On solving and taking ensemble average, we get

$$\begin{aligned}\langle|\psi_s|^2\rangle = |\psi_{s0}|^2 + \psi_{s0}\langle\psi_{s1}^*\rangle + \psi_{s0}\langle\psi_{s2}^*\rangle + \langle\psi_{s1}\rangle\psi_{s0}^* + \langle|\psi_{s1}|^2\rangle \\ + \langle\psi_{s1}\psi_{s2}^*\rangle + \psi_{s0}^*\langle\psi_{s2}\rangle + \langle\psi_{s1}^*\psi_{s2}\rangle + \langle|\psi_{s2}|^2\rangle\end{aligned} \tag{4.4}$$

Here, the terms containing $\langle\psi_{s1}\rangle$ or $\langle\psi_{s1}^*\rangle$ become zero due to the assumption of zero mean random rough surface, i.e., $\overline{f(x)} = 0$. Hence, we get

$$\langle|\psi_s|^2\rangle = |\psi_s|^2 + \psi_{s0}\langle\psi_{s2}^*\rangle + \langle|\psi_{s1}|^2\rangle + \psi_{s0}^*\langle\psi_{s2}\rangle + \langle\psi_{s1}\psi_{s2}^*\rangle + \langle\psi_{s1}^*\psi_{s2}\rangle + \langle|\psi_{s2}|^2\rangle \tag{4.5}$$

The reflection coefficient, r, is defined as the ratio of the reflected power divided by the incident power. On assuming amplitude of the incident field as unity, the reflection coefficient is given by

$$r = \langle|\psi_s|^2\rangle$$

4.2 Circular Polarisation Ratio (CPR)

"The circular-polarization ratio, μ is defined as the ratio of the echo power in the same circular polarisation state (SC) to that in the opposite circular polarisation state (OC)" [9].

$$\mu = \frac{\text{Same Circularly Polarise (SC)}}{\text{Opposite Circularly Polarise (OC)}} \tag{4.6}$$

4.3 Analysis using Radar Cross Section

Scattering pattern from a surface is highly dependent on its configuration. There may be multiple bounces before the signal reach back to the radar. So, each surface has different reflection co-efficient, i.e., radar cross section. In this section, we will analyse two icy surface configurations on the basis of RCS. In general, the radar used in remote sensing are monostatic. In a monostatic radar system, transmitter and receiver are collocated. So, the radar will receive the signal scattered in the direction exactly opposite to the incident field direction, i.e., scattering angle will be equal to the negative of the incident angle, i.e., $\theta_s = -\theta_i$.

4.3.1 Random Rough Surface

Let us assume a TE polarised wave of unit magnitude is incident on a icy random rough surface with Gaussian auto correlation function and small surface height as shown in Fig. 4.1. As we are assuming monostatic radar system, the signal received by the radar will be the signal scattered at scattering angle equals to $-\theta_i$. Zeroth and Second orders give scattering field in specular direction only. So, only first order will contribute to the direct backscatter to radar from the random rough surface, which can be calculated by substituting $\theta_s = -\theta_i$ in Eq (3.35). On substituing, we get

$$P_{BS} = 2\frac{k^2h^2l}{\sqrt{\pi}}\cos^2\theta_i \ |\chi|^2 \exp(-k^2l^2\sin^2\theta_i) \tag{4.7}$$

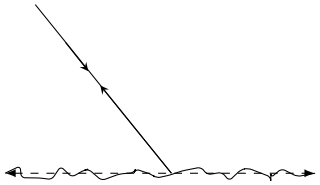

Figure 4.1: Backscattering phenomenon from random rough surface

where,

$$\chi = \frac{\cos\theta_i - \sqrt{\epsilon_r - \sin^2\theta_i}}{\cos\theta_i + \sqrt{\epsilon_r - \sin^2\theta_i}}$$

The variation of backscatter power from random rough surface as a function of the incident angle, i.e., monostatic radar viewing angle for a TE polarised incident wave is shown in Fig. 4.2.

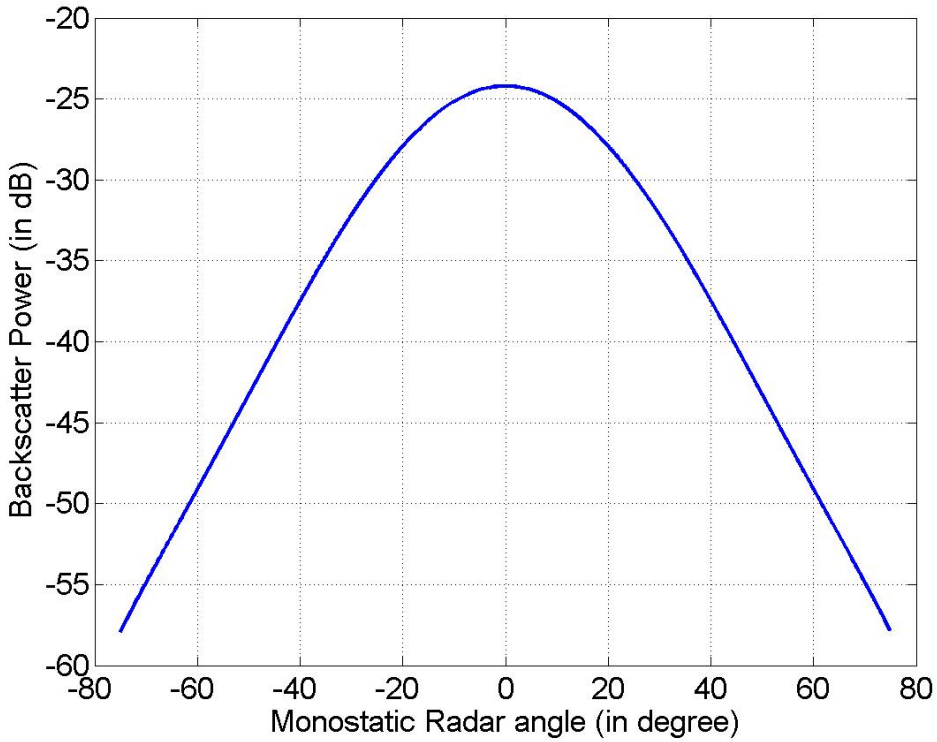

Figure 4.2: Backscatter Power variation as a function of Monostatic Radar viewing angle for TE polarisation.

Similarly, for TM polarisation, on substituting $\theta_s = -\theta_i$ in Eq (3.37). we get

$$\langle P_{BS} \rangle = 2\frac{k^2h^2l}{\sqrt{\pi}} \left| \frac{(\epsilon_r - 1)\cos\theta_i(\sin^2\theta_i(1-\epsilon_r) - \epsilon_r)}{(\epsilon_r\cos\theta_i + \sqrt{\epsilon_r - \sin^2\theta_i})^2} \right|^2 \exp(-k^2l^2sin^2\theta_i) \quad (4.8)$$

The variation of backscatter power from random rough surface as a function of the incident angle, i.e., monostatic radar viewing angle for an TM polarised incident

wave is shown in Fig. 4.3.

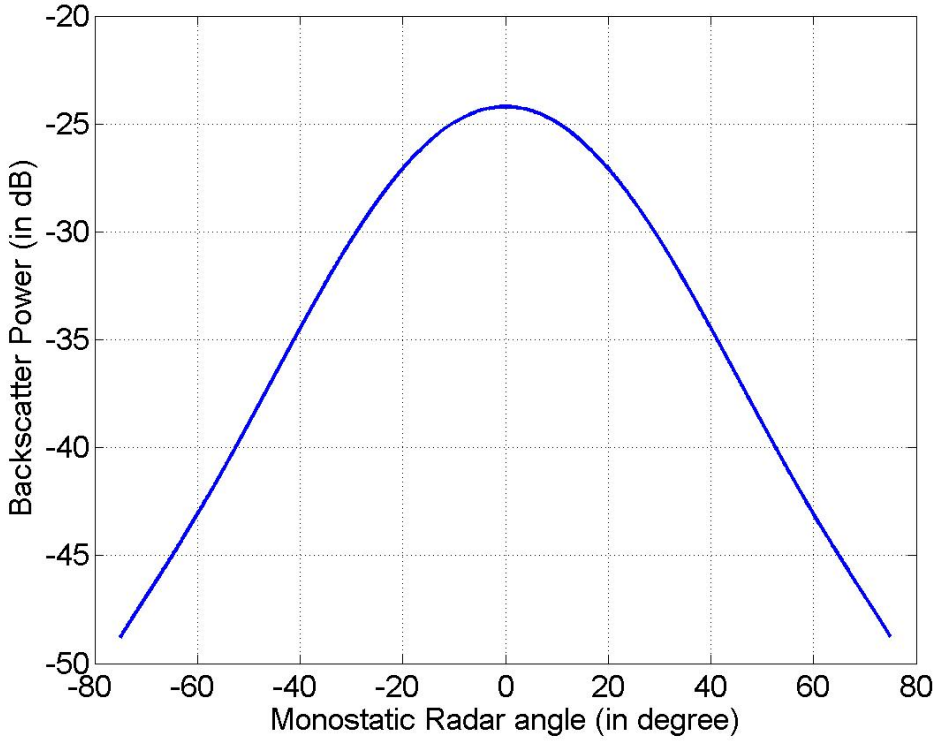

Figure 4.3: Backscatter Power variation as a function of Monostatic Radar viewing angle for TM polarisation.

4.3.2 Random Rough Surface with Boulders

Now, let us assume an icy random rough surface with smooth faced boulder as shown in Fig. 4.4. In this configuration, two types of scattering phenomena will occur. One will be the direct backscatter from random rough surface and another will be the double bounce through boulder as shown in Fig. 4.4 as case 1 and 2, respectively.

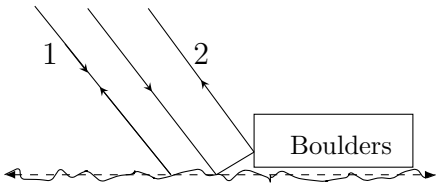

Figure 4.4: Backscattering phenomena from random rough Surface with smooth boulder

In previous section, we have already derived the expression for direct backscatter power from the random rough surface (case 1). In this section, we will derive the

expression for the backscatter power due to double bounce through boulder (case 2).

Firstly, we calculate the total power scattered in specular direction ($\theta_s = \theta_i$). And then we multiply it with the Fresnel reflection coefficient, as we have assumed smooth faced boulder, to get the backscatter field after double bounce through boulder.

The reflected power in specular direction will be given by

$$P_{specular} = (\psi_{s0} + \psi_{s1} + \psi_{s2})(\psi_{s0} + \psi_{s1} + \psi_{s2})^*|_{\theta_s=\theta_i}$$

On simplifying and taking ensemble average, we get

$$\langle P_{specular} \rangle = |\psi_{s0}|^2 + \psi_{s0}\langle\psi_{s2}^*\rangle + \langle|\psi_{s1}|^2\rangle + \langle\psi_{s2}\rangle\psi_{s0}^* + \langle|\psi_{s2}|^2\rangle \tag{4.9}$$

Here, we neglect $\langle|\psi_{s2}|^2\rangle$, due to complexity of its computation. So, on substituting $\theta_s = \theta_i$ in Eqs. (3.30), (3.35) and using these equations and Eq (3.21) in above equation, we get

$$\langle P_{specular} \rangle = |\chi|^2 + \chi\tilde{\psi}_{s2}^* + 2\frac{k^2h^2l}{\sqrt{\pi}}\cos^2\theta_i \;\; |\chi|^2 + \chi^*\tilde{\psi}_{s2} \tag{4.10}$$

Now, we multiply $\langle P_{specular} \rangle$ by Fresnel reflection co-efficient with incident angle $90 - \theta_i$. So, the backscatter power after the double bounce, P_{DB}, is given by

$$\langle P_{DB} \rangle = \langle P_{specular} \rangle \times |\chi_1|^2 \tag{4.11}$$

where,

$$\chi_1 = \frac{\sin\theta_i - \sqrt{\epsilon_r - \cos^2\theta_i}}{\sin\theta_i + \sqrt{\epsilon_r - \cos^2\theta_i}}$$

Now, let us assume a plane wave is incident on a random rough surface of length L with uniformly distributed smooth square boulders of size S, the scattered power for a 2-D scattering geometry (1-D surface) is given by

$$\langle P \rangle = \begin{cases} \frac{\langle P_{BS}\rangle(L - nS(1+\tan\theta_i)) + 2\;\; nS\tan\theta_i\langle P_{DB}\rangle}{L}, & 0 \le \frac{nS}{L} \le \frac{1}{1+2\tan\theta_i} \\ \frac{(\langle P_{BS}\rangle + 2\langle P_{DB}\rangle)(L - nS(1+\tan\theta_i))}{L}, & \frac{1}{1+2\tan\theta_i} \le \frac{nS}{L} \le \frac{1}{1+\tan\theta_i} \\ 0, & \frac{1}{1+\tan\theta_i} \le \frac{nS}{L} \le 1 \end{cases}$$

where,

$\langle P_{BS} \rangle$ = Ensemble averaged direct backscatter power from random rough surface,
$\langle P_{DB} \rangle$ = Ensemble averaged backscatter power after double bounce through random rough surface and the boulder,
n = Number of boulders,

and

$$\text{Boulder factor}(\alpha) = \frac{\text{Length covered by boulders}}{\text{Total Length}} = \frac{nS}{L}$$

Here, the factor of $\tan\theta_i$ is coming due to consideration of shadows of the boulder on the surface and a factor of 2 is due to the consideration of symmetry. i.e., there will be two cases of double bounce: field falls on vertical face of the boulder after reflection from the random rough surface and the field falls on the random rough surface after reflection from the vertical face of the boulder.

The boulder factor (α) is basically defining how much fraction of the surface is covered with the boulders. On substituting, $nS/L = \alpha$, we get

$$\langle P\rangle = \begin{cases} \langle P_{BS}\rangle(1-\alpha(1+\tan\theta_i)) + 2\alpha\tan\theta_i\langle P_{DB}\rangle, & 0 \le \alpha \le \frac{1}{1+2\tan\theta_i} \\ (\langle P_{BS}\rangle + 2\langle P_{DB}\rangle)(1-\alpha(1+\tan\theta_i)), & \frac{1}{1+2\tan\theta_i} \le \alpha \le \frac{1}{1+\tan\theta_i} \\ 0, & \frac{1}{1+\tan\theta_i} \le \alpha \le 1 \end{cases}$$

The variation in backscatter power as a function of the boulder factor, α, for TE polarised wave incident at an incident angle of 40° w.r.t. normal of the surface is shown in Fig. 4.5.

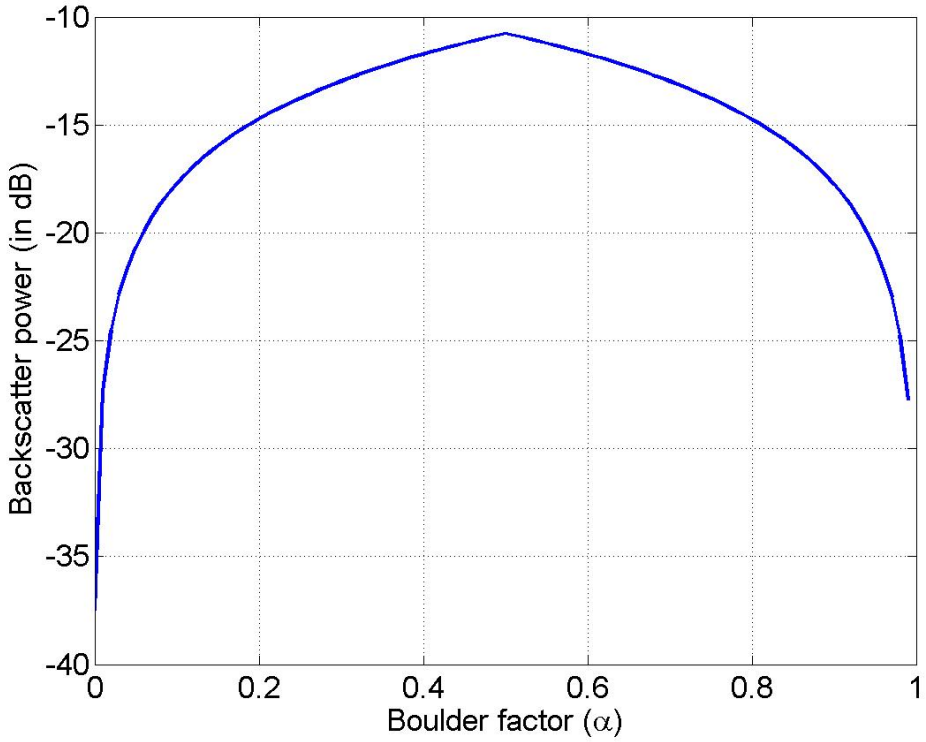

Figure 4.5: Backscatter Power variation as a function of Boulder factor (α) for TE polarisation at an incident angle of 40°.

4.4 Analysis using CPR

In section 3.2, we saw that the reflection coefficient for TE and TM polarised waves were different. Which implies that the reflection coefficient for the horizontal and

vertical components, $\hat{h}$ and $\hat{v}$ component, respectively, will be different. A circularly polarised field can be written as the superposition of horizontal and vertical linearly polarised field components. As the reflection coefficients are different for horizontal and vertical field components, the amplitude of the horizontal and vertical components in scattered field will be different and scattered field will not remain as circularly polarised. Due to different amplitudes of the horizontal and vertical field components, the resulting scattered field will be elliptically polarised. By the principle of orthogonality, we know that an elliptically polarised field can be written as the superposition of RHCP (Right Handed Circularly Polarised) and LHCP (Left Handed Circularly Polarised) field components. This will provide us the ratio of same sense of circularly polarised (SC) and opposite sense of circularly polarised field components, which is known as circular polarisation ratio.

Relation between reflection coefficients of Electric and Magnetic field components of a transverse wave -

By the principle of Fresnel reflection [15], we know that

$$\frac{E_i}{H_i} = -\frac{E_r}{H_r}$$

So,

$$\frac{E_r}{E_i} = -\frac{H_r}{H_i}$$

where,

E_i, H_i = electric and magnetic field component of the incident field, respectively
E_r, H_r = electric and magnetic field component of the reflected field, respectively
r_{TM} = Reflection coefficient of Magnetic field component of a TM wave

So, the reflection coefficient for the electric field component of a TM polarised wave with r_{TM} being the reflection coefficient for the magnetic field component will be given by $-r_{TM}$.

Now, let us assume the incident field is circularly polarised electric field. So, the reflection coefficient for the horizontal and vertical component will be given by r_{TE} and $-r_{TM}$, respectively.

Now, we will analyse two types of icy surfaces: random rough surface and random rough surface with uniformly distributed square smooth boulders, on the basis of the CPR.

4.4.1 Random Rough Surface

Let a RHCP (Right Handed circularly Polarised) electric field with propagation vector $\hat{k} = \hat{h} \times \hat{v}$ be incident on a random rough surface as shown in Fig. 4.6. The incident field can be written as:

$$\psi_{inc} = a(\hat{h} + j\hat{v})$$

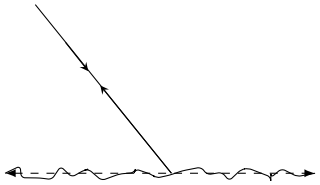

Figure 4.6: An RHCP electric field is incident on a random rough surface.

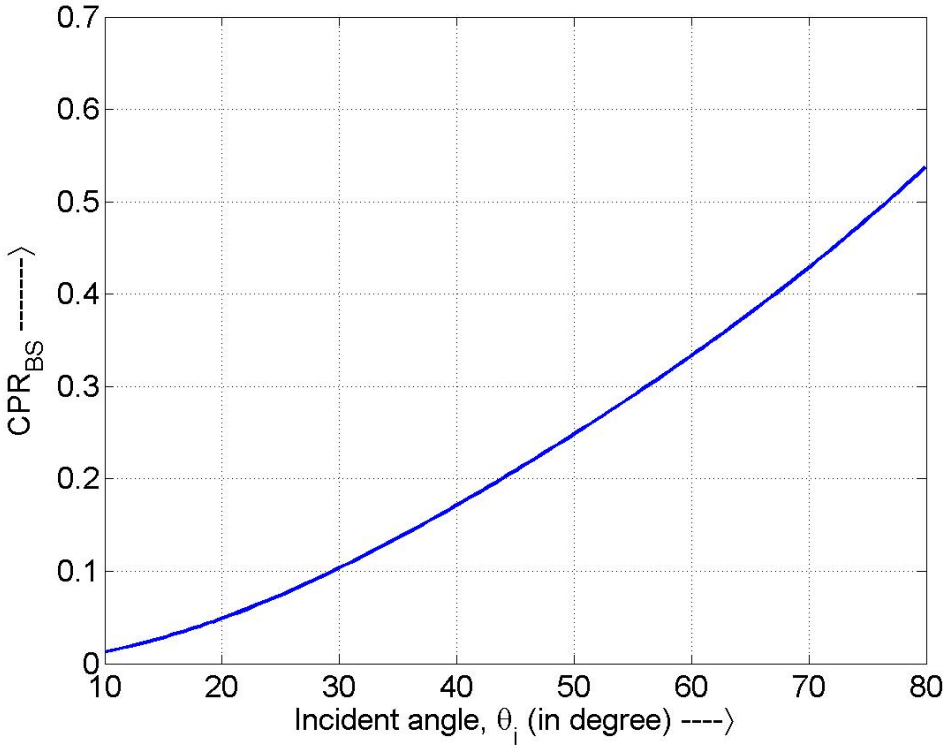

Figure 4.7: The variation of the backscatter CPR from random rough surface with incident angle w.r.t. normal to the surface.

On scattering from the surface, the horizontal component, $\hat{h}$ gets multiplied by r_{TE} and the vertical component, $\hat{v}$ gets multiplied by $-r_{TM}$ as described in section 4.4. Hence, the scattered field, ψ_s is given by

$$\psi_s = a(r_{TE}(\theta_i, \theta_s)\hat{h} - j \;\; r_{TM}(\theta_i, \theta_s)\hat{v}) \tag{4.12}$$

with propagation vector $\hat{k} = \hat{v} \times \hat{h}$. On rewriting the above equation, we get

$$\psi_s = a\frac{(r_{TE}(\theta_i, \theta_s) - r_{TM}(\theta_i, \theta_s))}{2}(\hat{h} + j\hat{v}) + a\frac{(r_{TE}(\theta_i, \theta_s) + r_{TM}(\theta_i, \theta_s))}{2}(\hat{h} - j\hat{v})$$

Here, first and second terms are giving the LHCP (Left Handed Circularly Polarised) and RHCP (Right Handed Circularly Polarised) components of the scattered field, respectively. As we have assumed that the incident field is RHCP polarised, RHCP component of the scattered field is the same sense circularly polarised field (SC) and

LHCP is the opposite sense circularly polarised field (OC). So, the CPR is given by

$$CPR = \frac{r_{TE}(\theta_i, \theta_s) + r_{TM}(\theta_i, \theta_s)}{r_{TE}(\theta_i, \theta_s) - r_{TM}(\theta_i, \theta_s)} \tag{4.13}$$

For backscatter, $\theta_s = -\theta_i$. So, the backscatter CPR, CPR_{BS} is given by

$$CPR_{BS} = CPR|_{\theta_s = -\theta_i}$$

The variation of the CPR_{BS} as a function of the incident angle w.r.t. normal is shown in Fig. 4.7.

4.4.2 Random Rough Surface with Uniformly Distributed Smooth Square Boulders

Now, let us assume that there is a smooth square boulder over the random rough surface as shown in Fig. 4.4. As discussed in previous section, there will be double bounce in this case, one from the random rough surface and another will be from the boulder face.

Using Eq.(4.12), scattered field from the surface is given by

$$\psi_s = a(r_{TEs}(\theta_i, \theta_s)\hat{h} - j \;\; r_{TMs}(\theta_i, \theta_s)\hat{v}) \tag{4.14}$$

where,

r_{TEs} = Reflection coefficient for TE polarise component from surface
r_{TMs} = Reflection coefficient for TM polarise component from surface

Due to smooth faced boulders, only specular field will go back to the radar. So, the scattering angle will be equal to the incident angle, i.e., $\theta_s = \theta_i$. Now scattered field will be the function of incident angle, θ_i only.

$$\psi_s(\theta_i) = a(r_{TEs}(\theta_i)\hat{h} - j \;\; r_{TMs}(\theta_i)\hat{v}) \tag{4.15}$$

with propagation vector, $\hat{k} = \hat{v} \times \hat{h}$. Now, let this field fall on the perpendicular face of the boulder. As we are assuming, smooth square perpendicular boulder, the scattered field from the surface will make $90 - \theta_i$ incident angle with the normal to the perpendicular face of the boulder. As boulder faces are smooth, the reflection co-efficient will be given by zeroth order term or the Fresnel reflection coefficient. So, the backscatter field after double bounce with propagation vector $\hat{k} = \hat{h} \times \hat{v}$ will be given by

$$\psi_s(\theta_i) = a(r_{TEs}(\theta_i) \;\; r_{TEb}(90 - \theta_i)\hat{h} + j \;\; r_{TMs}(\theta_i) \;\; r_{TMb}(90 - \theta_i)\hat{v}) \tag{4.16}$$

where,

r_{TEb} = Reflection coefficient for TE polarise component from boulder
r_{TMb} = Reflection coefficient for TM polarise component from boulder

On rewriting the above equation, we get

$$\psi_s(\theta_i) = a\frac{r_{TEs}(\theta_i)\ r_{TEb}(90-\theta_i) + r_{TMs}(\theta_i)\ r_{TMb}(90-\theta_i)}{2}(\hat{h}+j\hat{v}) + j\ a\frac{r_{TEs}(\theta_i)\ r_{TEb}(90-\theta_i) - r_{TMs}(\theta_i)\ r_{TMb}(90-\theta_i)}{2}(\hat{h}-j\hat{v}) \tag{4.17}$$

Here, first and second terms are the RHCP and LHCP components of the backscatter field after double bounce through boulder, respectively. As we have assumed incident wave as RHCP, the CPR after double bounce, CPR_{DB} will be given by

$$CPR_{DB} = \frac{r_{TEs}(\theta_i)\ r_{TEb}(90-\theta_i) + r_{TMs}(\theta_i)\ r_{TMb}(90-\theta_i)}{r_{TEs}(\theta_i)\ r_{TEb}(90-\theta_i) - r_{TMs}(\theta_i)\ r_{TMb}(90-\theta_i)} \tag{4.18}$$

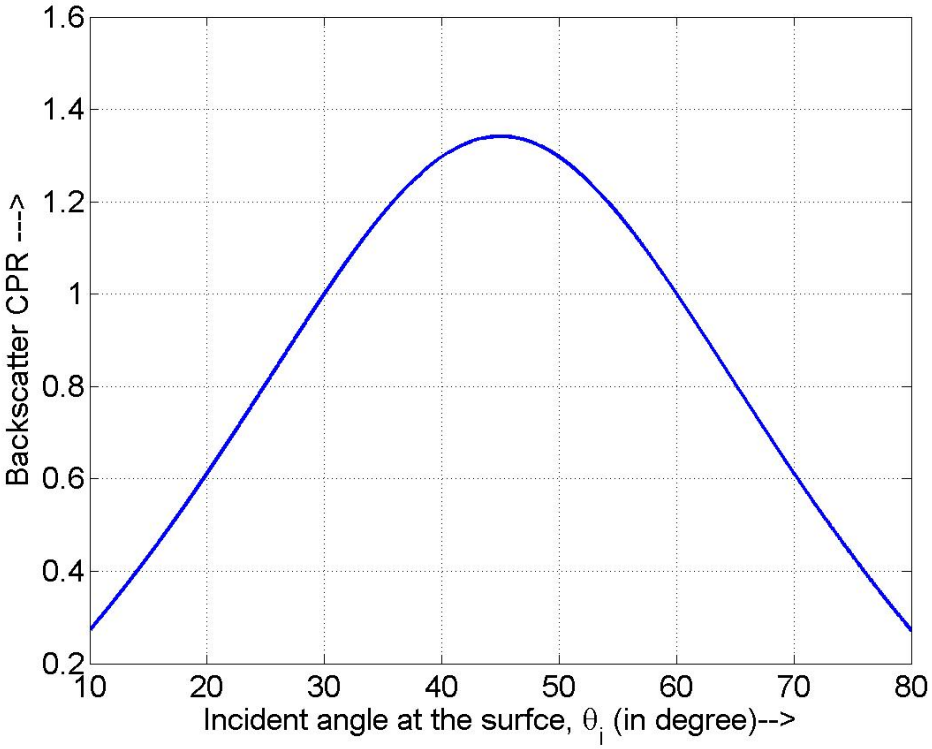

Figure 4.8: The variation in CPR w.r.t. the incident angle assuming both surface and boulder as smooth.

The above all expressions of CPR are valid only if various reflection coefficients are real and positive. If not, the above will change accordingly.

In Fig. 4.8, we have assumed both the surface and the boulder are smooth. Now the question arises, how the CPR will change, if the surface is randomly rough? To obtain its answer, we have plotted the variation in CPR after double bounce as a function of the randomness of the surface. In Fig. 4.9, we vary the rms height of the surface keeping correlation length constant. And in Fig. 4.10, we varied the correlation length keeping rms height of the surface constant.

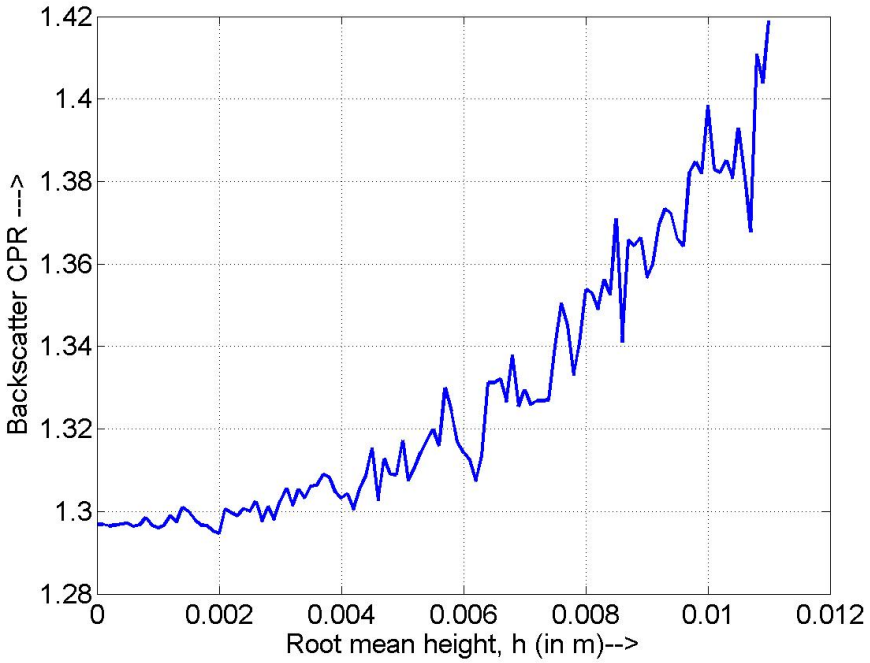

Figure 4.9: Variation in backscatter CPR from a random rough surface as a function of the rms height of the rough surface,h, keeping correlation length,l, constant.

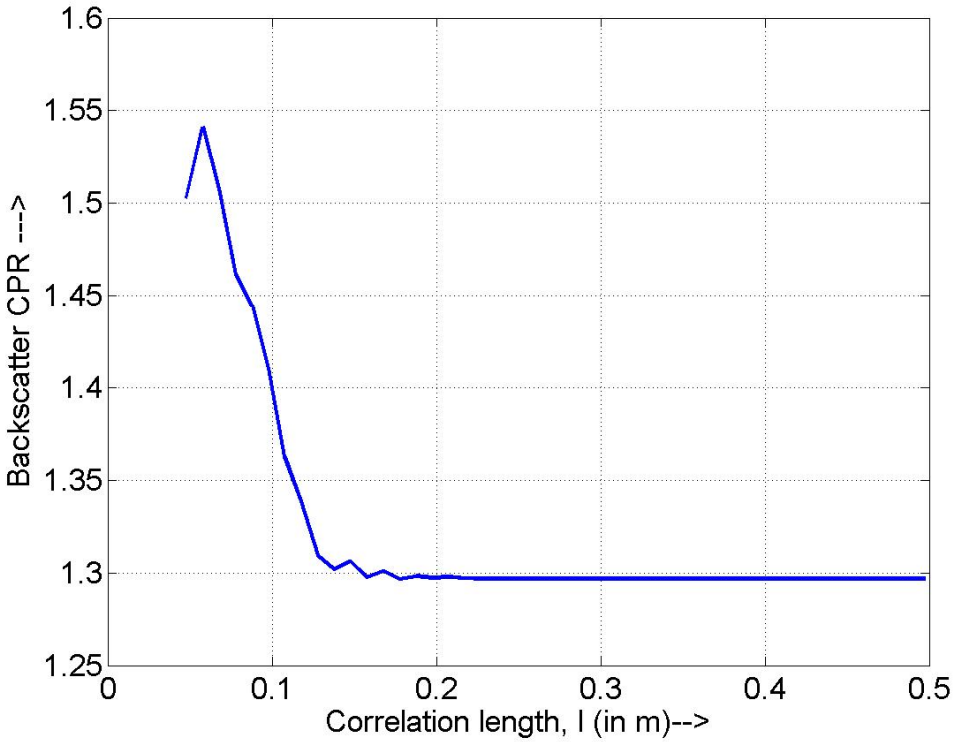

Figure 4.10: Variation in Backscatter CPR from a random rough surface as a function of the auto correlation length,l, of the rough surface keeping rms height,h, constant

Chapter 5

Conclusion

To understand the high radar albedo from the Enceladus (moon of the Saturn), we start with the analysis of the electromagnetic wave scattering from random rough surfaces. We used SPM (Small Perturbation Method) for the analysis and determined the scttered field expressions up to second order of perturbation. Further, we have analysed the various configurations of icy surfaces on the basis of RCS and CPR. In the analysis we have used incident angle equal to 40°, which is same as the incidence angle used by SMAP (Soil Moisture Active Passive) mission ot the JPL laboratory, NASA.

In chapter 2, we have analysed electromagnetic wave scattering from random rough surfaces. We continued the analysis in chapter 3, and derived the expressions for zeroth, first and second order scattered fields for both TE and TM polarised wave.

In zeroth order, for TE polarised wave, reflected power curve is like an upward parabola. Whereas, for TM polarisation, it has a null at the Brewster angle, $\theta_p = \tan^{-1}(n_2/n_1)$. We have done the analysis for icy surfaces with $\epsilon_r = 3$. So, the Brewster angle, $\theta_p = \tan^{-1}(\sqrt(3)) = 60°$. At $\theta_i = 0$, the reflected power for both the polarisations are same.

In first order, for TE polarised wave, the scattered power is more in the specular direction. Whereas, in TM polarisation, more power goes in the backscatter direction. The amplitude of oscillations are the function of the ratio of the correlation length, l and the surface length, L, i.e., l/L.

In chapter 4, we have analysed two types of surfaces: random rough surface and random rough surfaces with uniformly distributed smooth square boulders on the basis of RCS (Radar Cross Section) and CPR (Circular Polarisation Ratio). Backscatter power for a TE polarised wave at 40° incident angle is about -38 dB as shown in Fig. 4.2. And from Fig. 4.5, we have observed that there is about 25 dB variation in the backscatter power. Maximum backscatter power is about -11 dB at boulder factor, $\alpha = 0.5$.

Further, we have analysed the same surfaces using CPR and found very big varia-

tion in the values of CPR from the surface with boulder compared to the CPR from the rough surface. As shown in Fig. 4.7, the CPR from the random rough surface is around 0.18. Whereas, the CPR from the smooth surface with smooth square boulder is around 1.38 as shown in Fig. 4.8. Further, we observed a variation of about 0.12 on varying the roughness of the surface in case of double bounce at an incident angle of 40° keeping correlation length constant and a variation of about 0.24 in CPR on varying correlation length of the surface keeping rms height constant.

The analysis of icy surfaces on the basis of RCS and CPR shows that radar albedo and CPR goes to higher values due to presence of boulder like structures over the surface. This has very high priority on the surface of the Enceladus due to very small radius of the body (around 252 km) and the presence of the Cryovolcanoes. Due to small radius, the gravitational force over it is very less. Cryovolcanoes shoot geyser-like jets of water vapor, other volatiles, and solid material, including sodium chloride crystals and ice particles, into space, totaling approximately 200 kilograms (440 lb) per second. This lead to floating ice cubes over the surface of the Enceladus, which gives configuration similar to the random rough surface with boulders.

Appendix A

Green's Function and Its Gradient

"Green's function is defined as the field in a medium due to point source", i.e., it is it is the solution of the second order partial differential equation (Helmholtz equation), derived from the Maxwell's equation, where the driving force is a unit source (Dirac delta or impulse function).

$$\nabla^2 g(r, r') + \omega^2 \mu\epsilon \; g(r, r') = -\delta(r - r')$$

where ∇^2 is two dimensional Laplace operator, ω is the angular frequency of the wave, μ and ϵ are the magnetic permeability and electrical permittivity of the medium, respectively, $g(r, r')$ is the green's function and δ is the impulse function.

The solution of the above equation in cylindrical co-ordinate with incident field as cylindrical wave is given by the Hankel function. We have converted it to the rectangular co-ordinate with incident field as plane wave by the expansion method given by Cinotti [13]. On conversion we get

$$g(\overrightarrow{r}, \overrightarrow{r}') = \frac{i}{4\pi} \int_{-\infty}^{\infty} \frac{dk_x}{\sqrt{k^2 - k_x^2}} \exp\left[ik_x(x' - x) + ik_z|z' - z|\right]$$

Now, we have simplified it for both upper ($z' > f(x')$) and lower ($z' < f(x')$) dielectric mediums.

For region $z' < f(x')$,

$$g(\overrightarrow{r}, \overrightarrow{r}') = \frac{i}{4\pi} \int_{-\infty}^{\infty} dk_x \frac{1}{k_z} \exp[ik_x(x' - x) - ik_z(z' - z)] \tag{A.1}$$

and the gradient of the green's function is given by

$$\nabla g(\overrightarrow{r}, \overrightarrow{r}') = \frac{1}{4\pi} \int_{-\infty}^{\infty} \frac{1}{k_z} (k_x \hat{x} - k_z \hat{z}) \exp[ik_x(x' - x) - ik_z(z' - z)] dk_x \tag{A.2}$$

$$\sqrt{1 + (\frac{df}{dx})^2}\hat{n} \cdot \nabla g(\overrightarrow{r}, \overrightarrow{r}') = \frac{-1}{4\pi} \int_{-\infty}^{\infty} \left(\frac{df}{dx} \frac{k_x}{k_z} + 1 \right) \exp[ik_x(x' - x) - ik_z(z' - z)] \; dk_x \tag{A.3}$$

For region, $z' > f(x')$,

$$g_1(\overrightarrow{r}, \overrightarrow{r}') = \frac{i}{4\pi} \int_{-\infty}^{\infty} dk_{1x} \, \frac{1}{k_{1z}} \exp[ik_{1x}(x' - x) + ik_{1z}(z' - z)] \tag{A.4}$$

and the gradient of the green's function is given by

$$\nabla g_1(\overrightarrow{r}, \overrightarrow{r}') = \frac{1}{4\pi} \int_{-\infty}^{\infty} \frac{1}{k_{1z}} (k_{1x}\hat{x} + k_{1z}\hat{z}) \exp[ik_{1x}(x' - x) + ik_{1z}(z' - z)] \, dk_{1x} \tag{A.5}$$

$$\sqrt{1 + (\frac{df}{dx})^2}\hat{n} \cdot \nabla g_1(\overrightarrow{r}, \overrightarrow{r}') = \frac{1}{4\pi} \int_{-\infty}^{\infty} \left(\frac{-df}{dx} \frac{k_{1x}}{k_{1z}} + 1 \right) \exp[ik_{1x}(x'-x) + ik_{1z}(z'-z)] \, dk_{1x} \tag{A.6}$$

Appendix B

Auto Correlation Function of a Random Rough Surface

Auto correlation function of a variable defines the similarity of the variable with its own at different instant of time or space. Mathematically, Auto correlation, $R(\tau)$, of a variable function of time, $x(t)$, is given by

$$R(\tau) = \langle x(t_1)x(t_2)\rangle = \int_{-\infty}^{\infty} d\tau\ x(t)\ x(t+\tau)$$

This is the function of separation between the two observation points. So, we may define the auto correlation function of the random rough surface profile, $f(x)$, as

$$\langle f(x_1)f(x_2)\rangle = h^2 c(|x_1 - x_2|)$$

where h^2 is the rms height of the random rough surface. Here, we have described the correlation function of the various functions required in the analysis, which are as follows-

$$\langle F(k_{x1})F(k_{x2})\rangle = \frac{1}{4\pi^2}\int_{-\infty}^{\infty}\int_{-\infty}^{\infty}\langle f(x_1)f(x_2)\rangle \exp(-ik_{x1}x_1)\exp(-ik_{x2}x_2)\ dx_1dx_2 \tag{B.1}$$

$$= \frac{1}{4\pi^2}\int_{-\infty}^{\infty}\int_{-\infty}^{\infty} R(|x_1 - x_2|)\exp(-ik_{x1}x_1)\exp(-ik_{x2}x_2)\ dx_1dx_2 \tag{B.2}$$

Let $x_1 - x_2 = \sigma_1$ and $x_2 = \sigma_2$. So, $x_1 = \sigma_1 + \sigma_2$ and $dx_1dx_2 = d\sigma_1 d\sigma_2$

$$\langle F(k_{x1})F(k_{x2})\rangle = \frac{1}{4\pi^2}\int_{-\infty}^{\infty}\int_{-\infty}^{\infty} R(|\sigma_1|)\exp(-ik_{x1}\sigma_1)\exp(-i(k_{x1}+k_{x2})\sigma_2)\ d\sigma_1 d\sigma_2 \tag{B.3}$$

$$= W(k_{x1})\delta(k_{x1} + k_{x2}) \tag{B.4}$$

$$\langle ik_x F(k_x) * A_1(k_x)\rangle = \langle \int_{-\infty}^{\infty} dk\ i\tilde{A}_1(k) F(k-k_{ix})(k_x-k)F(k_x-k)\rangle \tag{B.5}$$

$$= \int_{-\infty}^{\infty} dk\ i\tilde{A}_1(k)(k_x-k)\ \langle F(k-k_{ix})F(k_x-k)\rangle \tag{B.6}$$

$$= \delta(k_x-k_{ix}) \int_{-\infty}^{\infty} dk\ i(k_x-k)\tilde{A}_1(k)\ W(k-k_{ix}) \tag{B.7}$$

Similarly, we get

$$\langle F(k_x) * A_1(k_x)\rangle\ = \delta(k_x-k_{ix}) \int_{-\infty}^{\infty} dk\ \tilde{A}_1(k)\ W(k-k_x) \tag{B.8}$$

$$\langle ik_x F(k_x) * F(k_x) * A_0(k_x)\rangle\ = \delta(k_x-k_{ix})\ i\tilde{A}_0 \int_{-\infty}^{\infty} dk\ (k_x-k)\ W(k-k_x) \tag{B.9}$$

$$\langle F(k_x) * F(k_x) * A_0(k_x)\rangle\ = \delta(k_x-k_{ix})\tilde{A}_0 \int_{-\infty}^{\infty} dk\ W(k-k_x) \tag{B.10}$$

$$\langle F(k_x) * B_1(k_x)\rangle\ = \delta(k_x-k_{ix}) \int_{-\infty}^{\infty} dk\ \tilde{B}_1(k)\ W(k-k_x) \tag{B.11}$$

$$\langle F(k_x) * F(k_x) * B_0(k_x)\rangle\ = \delta(k_x-k_{ix})\tilde{B}_0 \int_{-\infty}^{\infty} dk\ W(k-k_x) \tag{B.12}$$

Bibliography

[1] C. Elachi and J. J. Van Zyl, *Introduction to the physics and techniques of remote sensing*. John Wiley & Sons, 2006, vol. 28.

[2] U. Khankhoje, K. Mitchell, J. Castillo-Rogez, and M. Janssen, "Enceladus's brilliant surface: Radar modeling," in *Lunar and Planetary Science Conference*, vol. 44, 2013, p. 2531.

[3] K. Mitchell, U. Khankhoje, J. Castillo-Rogez, and S. Wall, "Enceladus' brilliant surface: Cassini radar observations and interpretation," in *Lunar and Planetary Science Conference*, vol. 44, 2013, p. 2902.

[4] S. O. Rice, "Reflection of electromagnetic waves from slightly rough surfaces," *Communications on pure and applied mathematics*, vol. 4, no. 2-3, pp. 351–378, 1951.

[5] K. F. Warnick and W. C. Chew, "Numerical simulation methods for rough surface scattering," *Waves in random media*, vol. 11, no. 1, pp. R1–R30, 2001.

[6] E. I. Thorsos, "The validity of the kirchhoff approximation for rough surface scattering using a gaussian roughness spectrum," *The Journal of the Acoustical Society of America*, vol. 83, no. 1, pp. 78–92, 1988.

[7] J. T. Johnson and J. D. Ouellette, "Polarization features in bistatic scattering from rough surfaces," *Geoscience and Remote Sensing, IEEE Transactions on*, vol. 52, no. 3, pp. 1616–1626, 2014.

[8] G. R. Valenzuela, "Depolarization of em waves by slightly rough surfaces," *Antennas and Propagation, IEEE Transactions on*, vol. 15, no. 4, pp. 552–557, 1967.

[9] B. A. Campbell, "High circular polarization ratios in radar scattering from geologic targets," *Journal of Geophysical Research: Planets*, vol. 117, no. E6, 2012.

[10] X. Gu, L. Tsang, H. Braunisch, and P. Xu, "Modeling absorption of rough interface between dielectric and conductive medium," *Microwave and Optical Technology Letters*, vol. 49, no. 1, pp. 7–13, 2007.

[11] W. C. Chew, *Waves and fields in inhomogeneous media*. IEEE press New York, 1995, vol. 522.

[12] K.-S. Chen, T.-D. Wu, L. Tsang, Q. Li, J. Shi, and A. K. Fung, "Emission of rough surfaces calculated by the integral equation method with comparison to three-dimensional moment method simulations," *Geoscience and Remote Sensing, IEEE Transactions on*, vol. 41, no. 1, pp. 90–101, 2003.

[13] G. Cincotti, F. Gori, M. Santarsiero, F. Frezza, F. Furno, and G. Schettini, "Plane wave expansion of cylidrical functions," *Optics communications*, vol. 95, no. 4-6, pp. 192–198, 1993.

[14] C. M. Bender and S. A. Orszag, *Advanced mathematical methods for scientists and engineers I.* Springer Science & Business Media, 1999.

[15] A. Kumar and A. K. Ghatak, *Polarization of light with applications in optical fibers.* SPIE Press, 2011, vol. 246.